Reconstitution of three-dimensional neuroepithelia from mouse and human pluripotent stem cells

D I S S E R T A T I O N

zur Erlangung des akademischen Grades
Doctor rerum naturalium
(Dr. rer. nat.)

vorgelegt

der Fakultät Mathematik und Naturwissenschaften
der Technischen Universität Dresden

von

Zhu, Yu
geboren am 14/07/1981 in Anhui, P.R. China

Gutachter:

Erster Gutachter: **Prof. Dr. Wieland B. Huttner**
Zweiter Gutachter: **Prof. Dr. Elena Cattaneo**

Eingereicht am:
Tag der Verteidigung:

CBG Max Planck Institute of Molecular Cell Biology and Genetics
CRTD Center for Regenerative Therapies Dresden
Dresden International PhD Program
Dresden International Graduate School for Biomedicine and Bioengineering
International Max Planck Research School for Molecular Cell Biology and Bioengineering
TECHNISCHE UNIVERSITÄT DRESDEN

Acknowledgements

I want to thank wholeheartedly my supervisor, Elly Tanaka, for giving me the opportunity to work on the fascinating topic of pluripotent stem cells in her family-like lab. I was very much impressed by Elly's never-ending motivation and enthusiasm for science, as well as her loud laughs every now and then. Her patient tutoring and enormous advice on shaping me not only as an experimentalist but also more importantly an independent researcher encouraged me to continue pursuing my long-term career goals.

I would like to give my special thanks to Andrea Meinhardt who was of tremendous help. I want to thank her for establishing neuroepithelial cyst model using mouse ES cells, helping me start human ES cell culture from zero in the lab, discussions on my project, as well as countless hours spent on guiding a foreigner like me to enjoy the life in Germany during these years.

I would like to thank Akira Tazaki for advice and technical support on the project. I also would like to express my gratitude to Marius Ader and Mike Karl for their advice on eye topics. Thanks to Kathleen Roensch for her kind help on *in situ* hybridization. Thanks go to Mike Tipsword for human RX and CRX antigen preparation.

I was very lucky to be working in a warm and funny lab, Tanaka lab, for my PhD. Many thanks go to all former and present members of the Tanaka lab for their many ideas, technical advice, and last but not least their clean or dirty jokes that make the experiments work better. Additionally, I would like to thank people in Huttner lab and Calegari lab for their valuable suggestions during our joint group meeting.

I'm grateful to my thesis advisory committee members Wieland Huttner and Francis Stewart for their advice and support.

I'm grateful to Wieland Huttner and Elena Cattaneo for agreeing to review this thesis.

I want to also thank the DIGS-BB Graduate Program for providing me financial support during my work on my doctoral thesis.

Finally, I would like to thank my families, especially my husband Xin Liang for all what he has done. No other words but thank you for his extreme support, encouragement, and unbelievable tolerance of my occasional vulgar moods! I thank my parents for believing all what I have done make sense and allowing me to be as ambitious as I wanted.

Summary

A current goal in pluripotent stem cell research is to reconstitute different aspects of embryonic development in defined conditions. The nervous system develops via formation of the neural tube--a pseudostratified epithelium with the apical cell surface oriented toward a single, central lumen. Cell diversification occurs through morphogen signaling along anterior-posterior and dorsal-ventral axes. Previous methods for generating neural cells from embryonic stem (ES) cell aggregates or embryoid bodies have resulted in complex often multi-lumen structures containing non-neural cells, rendering them too complex to be patterned by defined cues. In our lab, Andrea Meinhardt applied polarized epithelial cell culturing techniques to mouse ES cells and directly differentiated cells to neuroepithelial, pseudostratified "cysts" that stably harbor a single lumen. These cysts represent a starting point for reconstituting complex aspects of neural development in response to defined factors.

In this thesis, I focus on the reconstitution of neuroepithelia from mouse epiblast stem (EpiS) cells, human ES cells and human induced pluripotent stem (iPS) cells. By applying our neuroepithelial cyst model, I show that mouse EpiS cells, human ES and iPS cells all rapidly formed neuroepithelial cysts. Human ES cell-derived neuroepithelial cyst formation was dependent on Laminin and FGF and uniformly generated eyefield epithelial cysts by five days, a large acceleration over previous neural induction protocols and over human embryonic development. Further culturing of human eyefield epithelium either in the absence of growth factors or Activin A resulted in quantitative differentiation to neural retina or retinal pigment epithelium, respectively. This work describes a new *in vitro* model that allows the dissection of important cellular events during human development such as lumen formation, as well as signaling events required for human retinal development. The ability to efficiently and quantitatively make retinal pigment epithelium has strong implications for vision research.

Table of Contents

Chapter 4

List of Figures

List of Tables

List of Movies *(see the attached DVD)*

Abbreviations

ES	Embryonic Stem
EpiS	Epiblast Stem
iPS	Induced Pluripotent Stem
3D	Three-Dimensional
2D	Two-Dimensional
RPE	Retinal Pigment Epithelium
RPC	Retinal Progenitor Cell
EHS	Engelbreth-Holm-Swarm
MEF	Mouse Embryonic Fibroblast
MDCK	Madin-Darby Canine Kidney Cell
FGF	Fibroblast Growth Factor
IGF-1	Insulin-like Growth Factor 1
TGF-beta	Transforming Growth Factor beta
GFP	Green Fluorescent Protein
PH3	Phospho-Histone H3
EdU	5-Ethynyl-2'-Deoxyuridine
Ac	Activin A
Hr	Hour
RT-PCR	Reverse Transcription Polymerase Chain Reaction
DIGS-BB	Dresden International Graduate School for Biomedicine and Bioengineering

Chapter 1

Introduction

A goal in pluripotent stem cell research is the faithful differentiation to given cell types such as neural lineages. One specific aspect of neural induction is differentiation of pluripotent stem cells to retinal tissues including the neural retina and the retinal pigment epithelium (RPE). In this thesis, I sought to develop an *in vitro* model that could better resemble the *in vivo* developmental environment to reconstitute neuroepithelial from pluripotent stem cells and further study its potential applications in the eye field. This chapter will introduce the definition of pluripotent stem cells, *in vitro* neural differentiation of pluripotent stem cells based on current protocols, retinal development *in vivo* and retinal differentiation *in vitro*.

1.1 Pluripotent stem cells

Stem cells are a class of cells that can differentiate into diverse cell types and can self-renew to produce more stem cells. Pluripotent stem cells refer to stem cells that potentially can differentiate into any of the three germ layers: endoderm, mesoderm, or ectoderm. Pluripotent stem cells could give rise to any fetal or adult cell type, but not develop into a complete fetal or adult animal because they can not contribute to extraembryonic tissue, such as the placenta.

1.1.1 Embryonic stem cells

Embryonic stem (ES) cells are pluripotent stem cells derived from the inner cell mass of the blastocyst, an early-stage embryo. They can be maintained undifferentiated in culture and capable of unlimited proliferation *in vitro*. In 1981, ES cells were first derived from mouse embryos. In 1998, a breakthrough research in the field led by James Thomson occurred. They first developed a technique to isolate and grow human ES cells in cell culture(Evans and Kaufman, 1981; Martin, 1981; Thomson et al., 1998). Human ES cells differ significantly from mouse ES cells in their culture requirements, morphology, differentiation behavior, and molecular profile(Nichols and Smith, 2009).

1.1.2 Epiblast stem cells

The *in vitro* derivation of pluripotent stem cells from both embryonic and adult tissues holds tremendous promise for basic research and clinical applications. Access to pluripotency *in vitro* was thought to be limited to the derivation of ES cells from preimplantation blastocysts until recently. Reports of new pluripotent cell types including epiblast stem (EpiS) cells and induced pluripotent stem (iPS) cells opened a wider way for recent studies that evaluate the epigenetic and genetic mechanisms regulating a cell's acquisition of a pluripotent state.

EpiS cells are routinely isolated from the epiblast of early postimplantation rodent embryo(Bao et al., 2009; Brons et al., 2007; Tesar et al., 2007). Recently, Tesar group proved that EpiS cells could also be derived from pre-implantation mouse embryos. The preimplantation-derived EpiS cells exhibit molecular features and functional properties consistent with postimplantation-derived EpiS cells(Najm et al., 2011).

The mouse EpiS cells are distinct from the mouse ES cells in their epigenetic states and the signals controlling their differentiation. However, mouse EpiS cells and human ES cells share various characteristics, not only their growth factor dependence and their colony morphology, but also patterns of gene expression and signaling responses that normally function *in vivo(Bao et al., 2009; Brons et al., 2007; Najm et al., 2011; Tesar et al., 2007)*. It has always been researchers' concern that the unique properties of human ES cells, now seem to be shared with EpiS cells, could reflect a similar late epiblast origin.

1.1.3 Induced pluripotent stem cells

Induced pluripotent stem (iPS) cells are a type of pluripotent stem cell artificially derived from a non-pluripotent cell, typically an adult somatic cell, by transduction of several defined transcription factors. iPS cells were first generated in 2006 from mouse cells and in 2007 from human cells(Takahashi et al., 2007; Takahashi and Yamanaka, 2006; Yu et al., 2007). The derivation of iPS cells is crucially dependent on the genes used for the induction. Oct-3/4 and certain members of the Sox gene family have been identified as crucial transcriptional regulators involved in the induction of pluripotency. Additional genes, including certain members of the Klf

family, the Myc family, Nanog, and LIN28, have been identified to improve the induction efficiency. Successful reprogramming of differentiated somatic cells into a pluripotent state would make it possible to create patient- and disease-specific stem cells, showing great potential for regenerative medicine.

1.2 In vitro neural differentiation of pluripotent stem cells

The progress of human pluripotent stem cell research has laid the foundation for an emerging new field of biological research that holds promise to develop *in vitro* models of human development and disease, establish new platforms for discovering and testing drugs, and provide tools for the generation of cells and tissues for transplantation in clinic. With the availability of mouse and human ES, iPS cells, the challenge facing the field is the development of strategies for the generation of homogeneous populations of functional cell types, such as neural lineages, efficiently from pluripotent stem cells.

1.2.1 Two-dimensional neural differentiation of pluripotent stem cells

Differentiation along the neural lineage to obtain different neural cell types is one major endeavor in pluripotent stem cell research. Cells are typically differentiated in two-dimensional (2D) culture, passing through a rosette-forming neuroepithelial stage before maturing into later stage neural progenitor cells, or in various embryoid body/floating aggregate suspension cultures that are enriched for neuroepithelial cells before plating to generate 2D rosette cultures(Carpenter et al., 2001; Chambers et al., 2009; Elkabetz et al., 2008; Gerrard et al., 2005; Kim et al., 2010; Koch et al., 2009; Lamba et al., 2006; Pera et al., 2004; Reubinoff et al., 2001; Zhang et al., 2001). Rosette stage neuroepithelial cells are capable of broad differentiation potential along central nervous system and peripheral nervous system lineages in response to extrinsic signalings. However, the 2D culturing conditions do not resemble the natural three-dimensional environment of the neural tube stage during *in vivo* development, which to some extent might explain the low efficiency of differentiation outcome. Furthermore, a current limitation in embryoid body/floating aggregate suspension cultures as a starting point for neural differentiation is the heterogeneity, and ill-

defined organization of the suspended cells before differentiating to neuroepithelium upon exposure to defined culture conditions or via "self-organization". Thus, the efficiency for current 2D culturing-based strategies for neural differentiation of pluripotent stem cells remains to be largely improved.

1.2.2 Three-dimensional neural differentiation of pluripotent stem cells

Developed for a range of tissues including neural tissues the spatial organization of the cells takes into account, 3D cell culture models, in which cells being maintained in floating culture in the case of neural differentiation of pluripotent stem cells, serve to bridge the gap between *in vitro* studies and *in vivo* development. Eiraku et al. previously characterized neuroepithelium formation in high-density neurally induced aggregate cultures of mouse ES cells, which initially showed unorganized features and mixed composition in the first days of differentiation. These aggregates first formed a lumen or multiple lumina at 5 days that later transformed into multiple rosette-like structures within single aggregates. These complex, multi-rosette structures have been important for demonstrating the capacity of mouse ES cells to undergo corticogenesis. Application of high density aggregates to human ES cells resulted in lumen-containing neuroepithelial structures with layered cortical identity and structure in 46 days but the preceding morphogenesis of such structures has not been described(Eiraku et al., 2008). Recently the mouse high-density aggregate culture was further modified to induce eyecup morphogenesis after addition of low levels of Laminin and nodal to the culture medium. In this system, the aggregates contain eyefield, non-eyefield neuroepithelium and likely non-neural tissue, leading to complex inductive events followed by morphogenetic movements to form the optic cup(Eiraku et al., 2011).

1.2.3 Efficient neural differentiation from mouse ES cells using neuroepithelial cyst model

The *in vitro* reconstitution of 3D epithelial structure has been previously described for kidney and mammary epithelia, using Collagen I or Matrigel-based cultures that induce cells to develop apicobasal polarity and form a tight epithelium surrounding a single, central lumen(Inman and Bissell, 2010; Zegers et al., 2003). In our lab, Andrea

Meinhardt applied classical 3D epithelial cyst culture system to mouse ES cells (Figure 1.1 a). To form 3D neuroepithelial cysts she embedded mouse ES cells in Matrigel, a commercially available gelatinous extracellular matrix protein mixture, together with neural induction medium. Single mouse ES cells formed cysts clonally in Matrigel (Figure 1.1 a, b). Direct filming and subsequent wholemount immunofluorescence showed that clonal cysts formed a single lumen with apicobasal polarity as reflected in the luminally restricted expression of CD133 (also known as Prominin-1 in humans and rodents) (Figure 1.1 b, c). Mouse ES cell-derived cysts started to express the early neuroectodermal marker SOX1 at Day 5 (Figure 1.1 c) with the majority (82±16%) of the cysts acquiring $SOX1^+$ expression by Day 7. While epithelial cysts typically have a single cell-layered wall, we refer to the pseudostratified neuroepithelial structures we generate here as cysts, since they contain a single lumen and are therefore distinguishable from embryoid bodies or floating aggregates. Thus, Andrea proved that the Matrigel-based 3D culturing method efficiently supports the reconstitution of well-organized neural tube-like neuroepithelial tissue from mouse ES cells.

1.3 Retinal development in vivo and retinal differentiation in vitro

The retina is considered as part of the central nervous system, since it originates as outgrowth of the developing brain in vertebrate embryonic development. The retina consists of the outer retinal pigment epithelium layer and the juxtaposed neural retina that contains several layers of neurons interconnected with synapses (Figure 1.2).

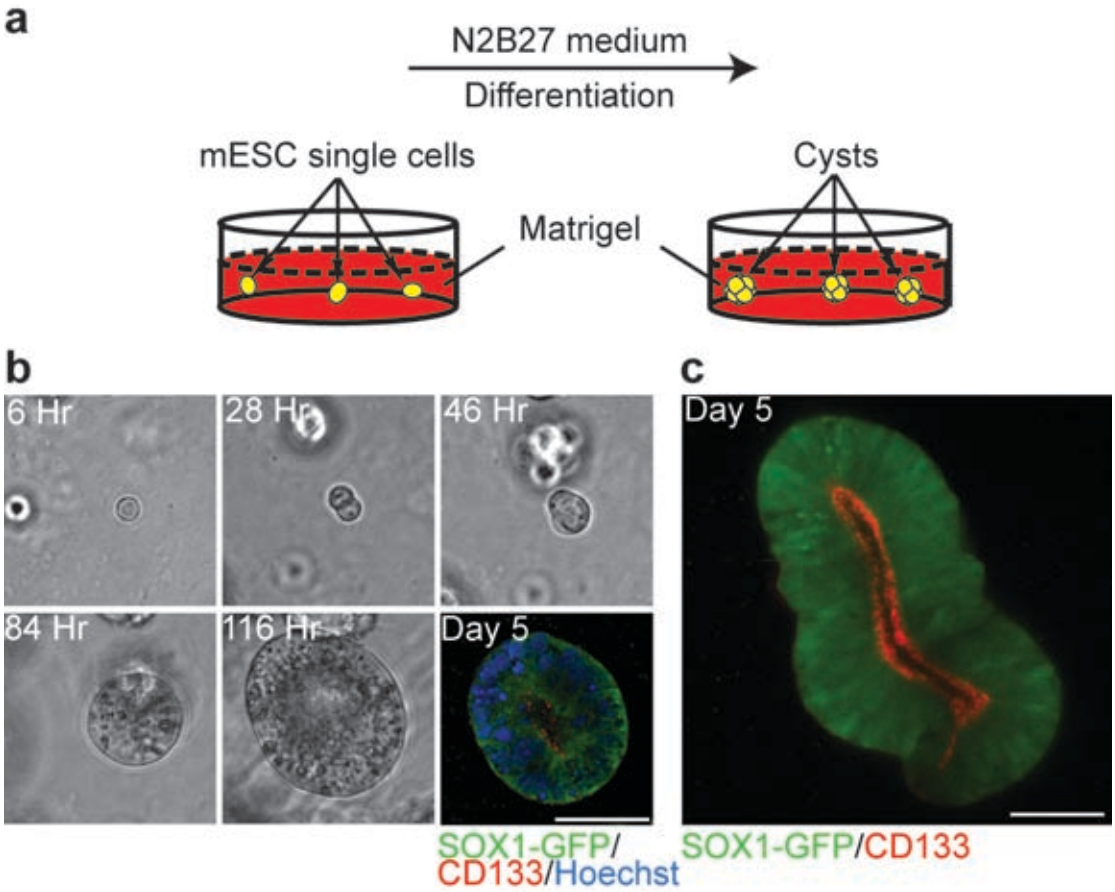

Figure 1.1 Efficient generation of neuroepithelial cysts from mouse ES cells in a Matrigel-based 3D culturing model.

(a) Schematic of the experiment. (b) Time-lapse phase contrast images showing an example of a single mouse ES cell that formed a sphere structure within 5 days. In the lower-right panel, Immunofluorescence of SOX1-GFP (green) and the restricted expression of CD133 (red) at the luminal side of this clonally formed sphere confirmed its neural identity and the presence of a single lumen. (c) A representative mouse ES cell-derived Day-5 cyst. Immunofluorescence of SOX1-GFP (green) and CD133 (red) outlined the apical lumen. Nuclei were counterstained with Hoechst. Hr: hours. Scale bar, 50 μm.

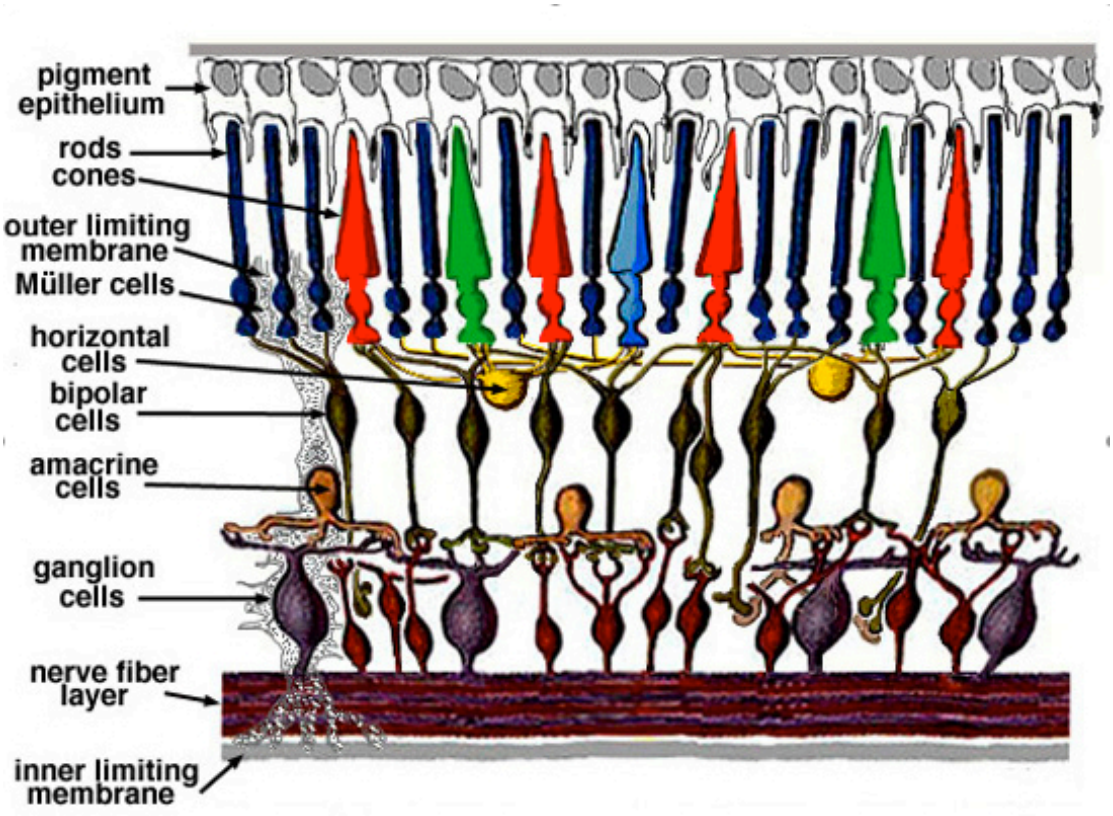

Figure 1.2 Layered structure of the vertebrate retina.

Schematic obtained from Webvision, The Organization of the Retina and Visual System.

1.3.1 Retinal development in vertebrates

A key factor in studying retinogenesis *in vitro* is to understand how it develops in the embryonic stages. The earliest stage to eye development is the formation of the paired optic vesicles on either side of the forebrain. The optic vesicle evaginates from the diencephalon, where it meets the surface ectoderm of the embryo. Upon contacting the surface ectoderm, it induces the formation of a lens placode, which then invaginates to form a lens vesicle and eventually becomes the mature lens. The optic vesicle itself undergoes simultaneous invagination process together with lens placode and forms the optic cup, whose two layers differentiate in different ways. The outer layer later gives rise to the retinal pigment epithelium, while the cells of the inner layer proliferate rapidly and generate a variety of glia, ganglion cells, interneurons, and light-sensitive photoreceptor neurons, which constitute the layered neural retina. (Figure 1.3)

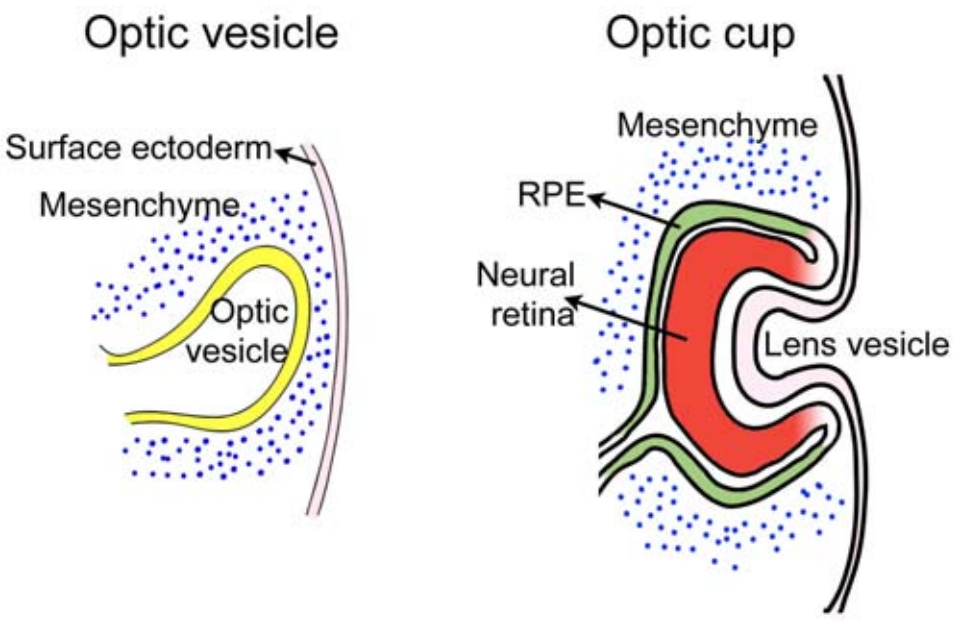

Figure 1.3 Schematic of two key stages during embryonic eye development in vertebrates.

How is it that a specific region of neural ectoderm is informed that it will become the optic vesicle? Several eyefield transcription factors --- *Six3*, *Pax6*, and *Rx* et al. --- are co-expressed in the anterior region of the vertebrate neural plate, which will later split into the bilateral regions forming the optic vesicles. Expression of an eyefield transcription factor cocktail with *Otx2* is sufficient to induce ectopic eyes even outside the nervous system. Previous reports support a model of progressive tissue specification in which neural induction regulated by a network of transcription factors, then *Otx2*-driven neural patterning primes the anterior neural plate for eyefield formation(Zuber et al., 2003).

1.3.2 Retinal differentiation from pluripotent stem cells

Retinal cells are particularly well-suited for the *in vitro* studies of cell differentiation and dysfunction based on pluripotent stem cell technology. The vertebrate retina develops and laminates via a defined series of events distinct on available diagnostic markers(Chow and Lang, 2001; Finlay, 2008; Hatakeyama and Kageyama, 2004; Marquardt and Gruss, 2002; Oliver and Gruss, 1997; Zhang et al., 2002). Furthermore, only one specific retinal cell class is often initially responsible for the effects of inherited and acquired retinal degenerative diseases, which simplifies the study of cellular mechanisms and potential therapies of the diseases.

Many groups worldwide have been working on the retinal differentiation from pluripotent stem cells by exposing them to different culture conditions. However, the current methods for differentiating human pluripotent stem cells into retinal progenitor cells, and further into differentiated cell types such as RPE or photoreceptor cells are inefficient and lengthy, limiting their effective use for *in vitro* basic research, transplantation and drug screening in regenerative medicine. For differentiation of cells into RPE, one of the earliest differentiated cells during retinal development, two different classes of protocols have been developed. One relies on random differentiation of human ES cells or iPS cells in serum- or serum-substitute containing media(Buchholz et al., 2009; Klimanskaya et al., 2004; Vugler et al., 2008). The rate of such cells that spontaneously differentiate into RPE cells is extremely low, less than 1%. The reason why some cells turn into RPE cells while others do not is unclear. The RPE cell clones are then picked up manually and

expanded, a process that takes at least six weeks. The other class of protocols starts by forming floating aggregates. Several methods starting with floating aggregates have reported 10-34% efficiency in 4-17 weeks, representing a substantial improvement yet selection is still required to obtain a uniform RPE cell layer (See table 1.1). In general, the current procedures to produce retinal cells from pluripotent stem cells have many disadvantages. They take many weeks to obtain differentiated cells and their efficiency is very low(Buchholz et al., 2009; Hu et al., 2010b; Idelson et al., 2009; Klimanskaya et al., 2004; Lamba et al., 2006; Meyer et al., 2011; Meyer et al., 2009; Osakada et al., 2008; Vugler et al., 2008).

Manuscript	**Stem cell source**	**RPE or RPC**	**Essential method**	**Time**	**Efficiency**
Klimanskaya I et al. Vugler A et al.	Human, ES	RPE	Spontaneous differentiation	60 days	>1%
Buchholz DE et al.	Human, iPS	RPE	Spontaneous differentiation	60 days	>1%
Idelson M et al.	Human, ES	RPE	Floating aggregates +Activin and NIC	6 weeks	33%
Meyer JS et al.	Human	RPC, RPE	Floating aggregates	16 Days 40 Days	>95% Rx^+ 25% $Mitf^+$
Osakada F et al.	Primate, ES	RPC, RPE	Floating aggregate +DKK1 and Lefty (Human ES)	35 Days 50 Days 120 Days	16% Rx^+-$Pax6^+$ 31% $Mitf^+$-$Pax6^+$ 34% $ZO1^+$

Table 1.1 Published protocols of RPE generation from human pluripotent stem cells. RPC: retinal progenitor cell.

1.4 Aims of the study

1.4.1 Develop an in vitro 3D model for the efficient neural induction of mouse EpiS cells, human ES and iPS cells

3D differentiation models for pluripotent stem cells could better mimic the *in vivo* situation and thus often lead to better efficiency as discussed in Chapter 1.2. Andrea Meinhardt in our lab applied 3D epithelial cell culturing techniques onto mouse ES cells and successfully reconstituted neural tube-like structures containing lumen, named neuroepithelial cysts, from single mouse ES cells. I aim to study whether this neuroepithelial cyst model proved using mouse ES cells would also work for neural induction from mouse EpiS cells, human ES and iPS cells, which are distinct from mouse ES cells as discussed in Chapter 1.1.

1.4.2 Mechanisms involved in the high efficiency of neural induction in the in vitro 3D model

Which factors are crucial to support the high efficiency of neural induction from pluripotent stem cells in the neuroepithelial cysts model is of great interest and would contribute to make the differentiation conditions defined. I aim to study the mechanisms involved in this model from two points: basement membrane components and secreted signaling factors.

1.4.3 Further differentiation of neural progenitor cells generated in the in vitro 3D model using human ES cell system

The spatially organized neural progenitor cells generated with high efficiency in the neuroepithelial cyst model especially using human ES cell system open up the possibility of studying human embryonic development in the central nervous system *in vitro*. To investigate the potential applications of the neuroepithelial cyst model, I first aim to characterize the regional identity of human ES cell-derived neuroepithelial cyst in the central nervous system. Second, I aim to further differentiate these neural progenitor cells into more mature cell types under defined conditions to prove

whether they are susceptible to cell fate determination by inductive signalings and thus potentially patternable in 3D.

Chapter 2

Reconstitution of 3D neuroepithelia from mouse EpiS cells and human ES cells using the neuroepithelial cyst model

To test whether the Matrigel-based neuroepithelial cyst model developed in our lab using mouse ES cells would also support the efficient neural differentiation of mouse EpiS cells and human ES cells that represent a later developmental stage, I optimized the condition and applied the neuroepithelial cyst model onto both cell types and further address the issue that which factors determine cyst formation using human ES cell system.

2.1 Mouse EpiS cells efficiently form neuroepithelial cysts in Matrigel

2.1.1 Mouse EpiS cell culture

Mouse EpiS cells were cultured in Activin A and FGF2-containing medium on Fibronectin-coated plates. The cells grew as flat, compact colonies (Figure 2.1 a), which were morphologically distinct from rounded colonies of mouse ES cells. Immunostaining showed that these flat and compact colonies expressed the pluripotency markers OCT4 and SSEA1.

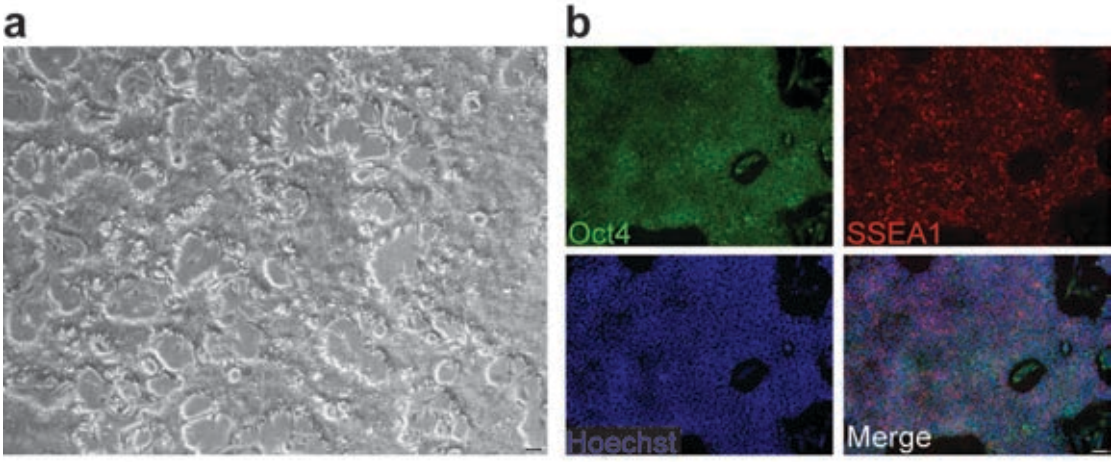

Figure 2.1 Mouse EpiS cells in culture.

(a) Phase contrast image of mouse EpiS cells cultured on Fibronectin-coated plate. (b) Immunostaining of pluripotency markers OCT4 (green), SSEA1 (red) on the mouse EpiS cell colonies. Nuclei were counterstained with Hoechst. Scale bar, 50 μm.

2.1.2 Mouse EpiS cell clumps form neuroepithelial cysts in Matrigel within 1 day

To form 3D neuroepithelial cysts I embedded mouse EpiS cells in Matrigel together with neural induction medium N2B27. Unlike mouse ES cells (see Figure 1.2 in Chapter 1), mouse EpiS cells did not form cysts from single cells. Instead, all mouse EpiS cell clumps reorganized and polarized to form neural tube like structures in Matrigel within 1 day (Figure 2.2 a). 97±2% of mouse EpiS cell-derived cysts were $SOX1^+$ at Day 1 (Figures 2.2 b). The apical distribution of CD133 and Phalloidin reflected the rapid cell polarization and formation of a single lumen within the growing cysts (Figure 2.2 b).

2.2 Human ES cells form uniform neuroepithelial cysts in Matrigel

2.2.1 Human ES cell culture

Basic techniques to culture human pluripotent stem cells are well established. Human ES cells were first derived and cultured on feeder cells such as mouse embryonic fibroblast (MEF) feeder layer(Thomson et al., 1998), though limitations remain in this traditional feeder-dependent culture method. In particular, the feeder-dependent culture method will hinder the development of clinical applications due to difficulty with quality control of undefined components provided by feeder cells. Therefore, a groundbreaking study in the field is the development of defined culture conditions that support the self-renewal of human pluripotent stem cells without the need for feeders. Several groups have developed culture conditions for human pluripotent stem cells that are feeder-free. In 2006, Ludwig and colleagues formulated mTeSR1 that is a standardized medium for long-term feeder-independent maintenance of human pluripotent stem cells and widely used nowadays(Ludwig et al., 2006a; Ludwig et al., 2006b).

To establish the culture techniques for human ES cells in our lab, I first tried to culture human ES cell line H9 on inactivated MEF feeder cells in knockout serum replacement-containing medium. However, H9 cells displayed frequent spontaneous

differentiation on MEF feeder layers, probably due to the improper mouse strain I used (BL6 mice). Then I moved on to the defined culture method for human pluripotent stem cells based on mTeSR1 that eventually works on several lines in our lab. Human ES cells were maintained in mTeSR1 on hESC-qualified matrix-coated plates. Cells grew in large, flat and compact colonies, similar to mouse EpiS cell colonies. Human ES cells were ready to passage when the colonies began to merge, and have centers that were dense compared to their edges (Figure 2.3 a). The undifferentiated state of human ES cells was confirmed by expression of pluripotency markers OCT4 and SSEA4 (Figure 2.3 b).

2.2.2 Human ES cell clumps form neuroepithelial cysts in Matrigel within 5 days

I next examined whether human ES cells could also be induced to faithfully reproduce neuroepithelial cell architecture (Figure 2.4 a). In Matrigel, all human ES cell clumps reorganized into cysts containing a single lumen within 24 hours (see Movie 2.1 in the attached DVD). Like the mouse EpiS cells, efficient cyst formation was not observed from single cells. Human ES cell-derived cysts displayed a neural tube-like structure with a smooth basal edge and an apical lumen (Figure 2.4 b). Immunostaining of whole-mount preparations followed by confocal microscopy showed that human ES cell-derived cysts were composed of polarized neural progenitors. At Day 1, all the cysts expressed NESTIN and SOX2 (Figure 2.4 c) while the early human neuroectodermal marker PAX6 was up-regulated gradually to be strongly expressed in 99±1% cysts by Day 5 (Figure 2.4 d, e). The apicobasal polarity of the cysts was reflected by the apically restricted distribution of CD133 and ZO-1 at apical junctions (Figures 2.4 c-e). The polarity is further depicted by luminal cell mitosis (Figure 2.4 f), which is an important feature of polarized neuroepithelial cells. These observations indicate that human ES cells form organized neural tube-like cysts in Matrigel within 5 days. The onset of neuroepithelial identity in this 3D model is accelerated over typical 2D cultures, and embryoid body-based induction protocols(Carpenter et al., 2001; Chambers et al., 2009; Eiraku et al., 2008; Elkabetz et al., 2008; Gerrard et al., 2005; Kim et al., 2010; Pera et al., 2004; Reubinoff et al., 2001; Zhang et al., 2001).

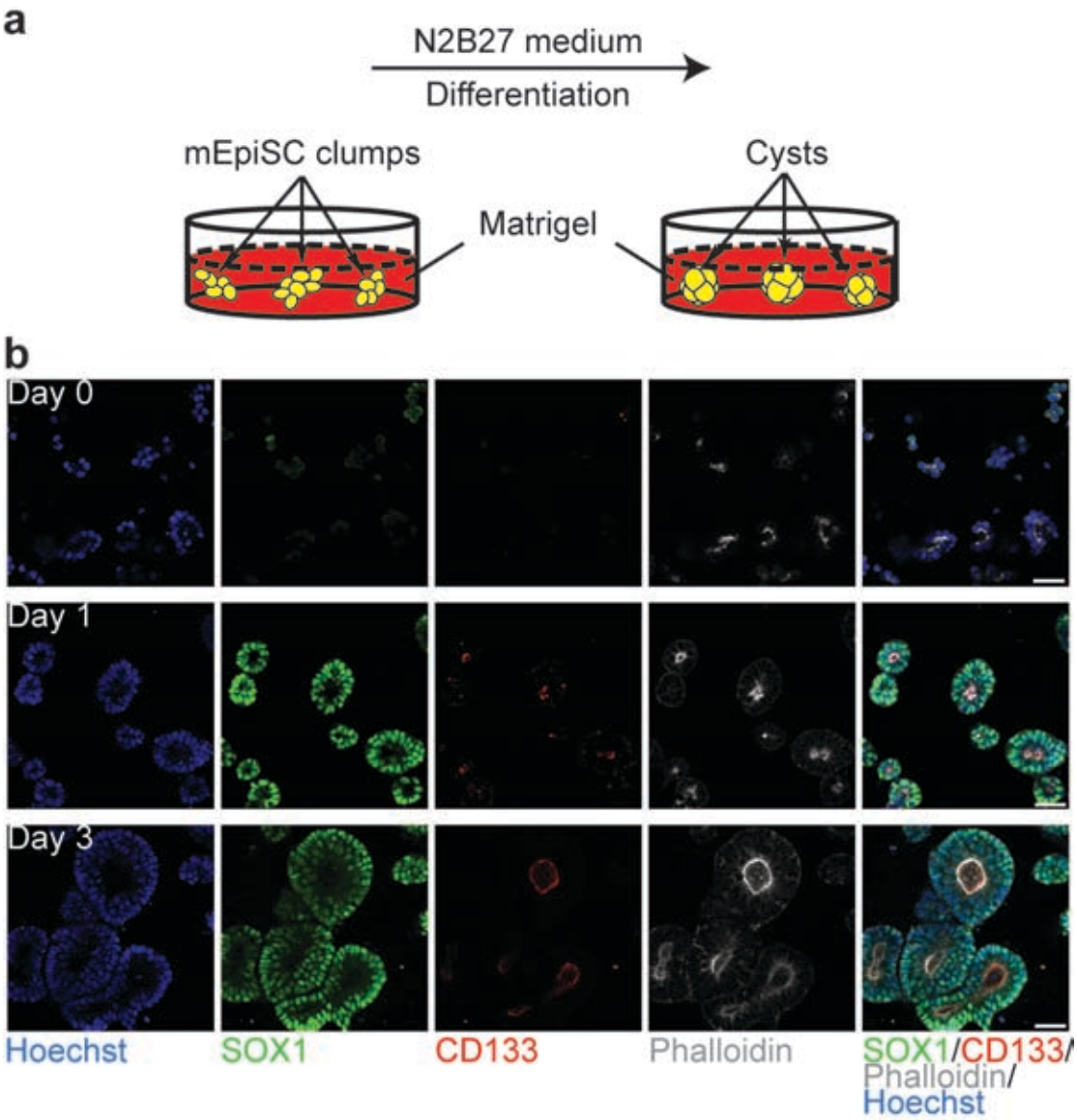

Figure 2.2 Efficient generation of neuroepithelial cysts from mouse EpiS cells in a Matrigel-based 3D culturing model.

(a) Schematic of the experiment. (b) Immunostaining of SOX1 (green), CD133 (red) and Phalloidin (white) during mouse EpiS cell-derived cyst growth in Matrigel. At Day 0 (samples were fixed 30 minutes after embedding) (top row), neuroepithelial cell marker SOX1 was negative in most cells. The tendency for stronger staining of Phalloidin at one side of the embedded cell clumps suggested that the cell polarity could be induced rapidly in the 3D neuroepithelial cyst model. At Day 1 shown in the middle row, all cell clumps formed cysts and became $SOX1^{+}$. Distribution of both CD133 and Phalloidin toward the apical side of the cysts indicated the apicobasal cell polarity. By Day 3 (bottom row), mouse EpiS cell-derived cysts grew bigger and were still positive for SOX1. Immunofluorescence of CD133 and Phalloidin clearly showed the single lumen in the formed cysts. Nuclei were counterstained with Hoechst. Scale bar, 50 μm.

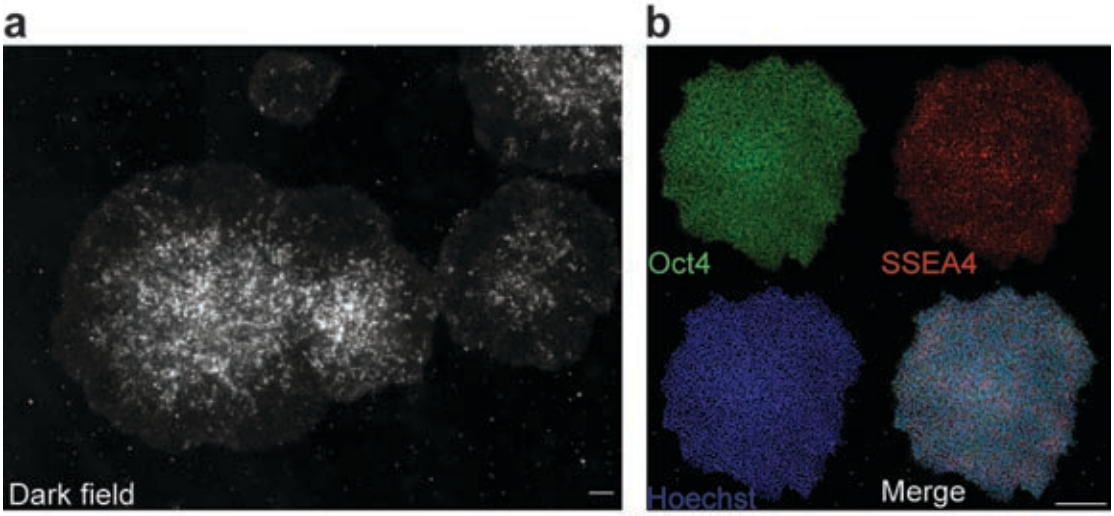

Figure 2.3 Human ES cells cultured in mTeSR.

(a) Morphology of undifferentiated human ES cell colonies cultured in mTeSR. (b) Immunostaining of pluripotency markers OCT4 (green), SSEA4 (red) on the human ES cells. Nuclei were counterstained with Hoechst. Scale bar, 200 μm.

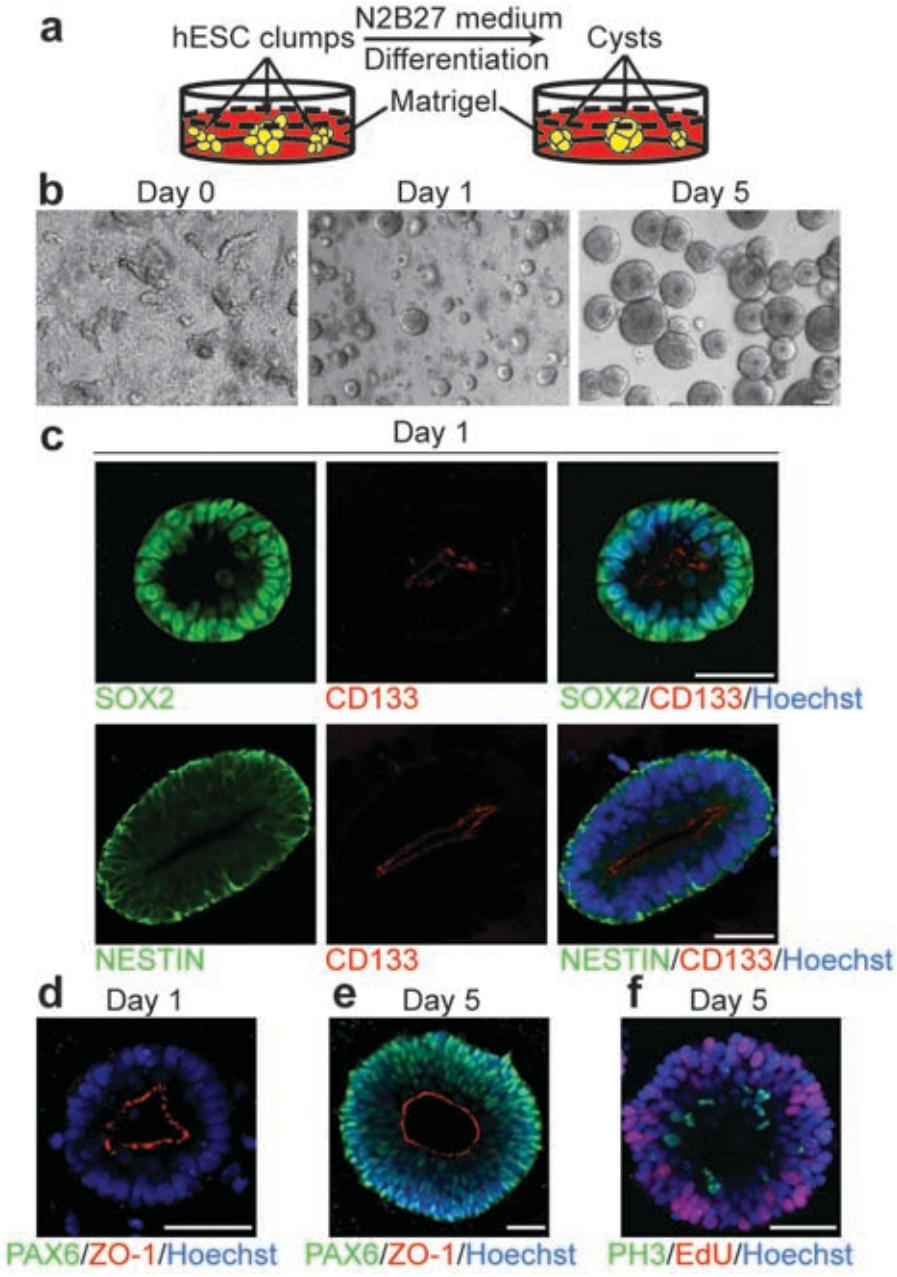

Figure 2.4 Efficient generation of polarized neural progenitors from human ES cells in the neuroepithelial cyst model.

(a) Schematic of the experiment. (b) Human ES cell clumps embedded in Matrigel at Day 0 formed cysts within 1 day. At Day 5, phase contrast image of human ES cell-derived cysts showed a single lumen inside. (c) By Day 1, human ES cell-derived cysts were positive for SOX2 (upper row, green) and NESTIN (lower row, green). The apical localization of CD133 (red) indicated apicobasal polarity was firmly established. (d, e) Immunostaining of PAX6 (green) and ZO-1 (red) during cyst growth in Matrigel. PAX6 was strongly expressed in Day-5 cysts that display clear properties of a pseudostratified epithelium. (f) M-phase cells stained with Phospho-Histone H3 (PH3) antibody only localized at apical side of the cysts and S-phase cells labeled with EdU at basolateral side, indicating luminal cell mitosis occurred within the cysts. Nuclei were counterstained with Hoechst. Scale bar, 50 μm.

2.3 Mechanisms involved in human ES cell-derived neuroepithelial cyst formation

2.3.1 Human ES cell-derived neuroepithelial cyst formation depends on Laminin

Using the highly efficient human ES cell-derived neuroepithelial cyst system I next sought to address the issue that which factors determine cyst formation.

Matrigel, used in our neuroepithelial cyst system, is a commercially available gelatinous protein mixture secreted by Engelbreth-Holm-Swarm (EHS) mouse sarcoma cells. This mixture resembles the complex extracellular environment found in many tissues and therefor is commonly used as a substrate for cell culture. Matrigel is rich in extracellular matrix proteins including Laminin, Collagen IV, Heparan sulfate proteoglycans, and Entactin/Nidogen(Kleinman et al., 1986; Kleinman et al., 1982). It also contains TGF-beta, epidermal growth factor, insulin-like growth factor, fibroblast growth factor, tissue plasminogen activator, and other growth factors that occur naturally in the EHS tumor(McGuire and Seeds, 1989; Vukicevic et al., 1992). Thus Matrigel is not a well-defined material.

To determine the basement membrane components required for neuroepithelial cyst induction I compared neuroepithelial cyst formation in Collagen I, Laminin/Entactin and Matrigel. Though Collagen I supports the *in vitro* kidney and mammary epithelial cyst formation(Inman and Bissell, 2010; Zegers et al., 2003), few human ES cell clumps (10±4%) formed cysts under these conditions (Figure 2.5 a, c). In contrast, a highly concentrated Laminin/Entactin gel (10 mg/ml), supported nearly all human ES cell clumps to form $PAX6^{+}$ neuroepithelial cysts with defined apicobasal polarity (96±3%), similar to that seen in Matrigel (95±5%) (Figure 2.5 a, c). Blockade of β1-integrin by the function-blocking antibody AIIB2, which reportedly blocks cell attachment to Laminin as well as Fibronectin, Collagen I and Collagen IV(Werb et al., 1989), significantly reduced cyst formation in Matrigel to 29±7% (Figure 2.5 b, c). These data suggest that Laminin, one of the major components in basal lamina, is required for efficient generation of neuroepithelial cysts.

2.3.2 Human ES cell-derived neuroepithelial cyst formation depends on FGF signaling

A second consideration was whether the 3D gels enhance the accumulation of secreted factors required for cyst formation. To test this issue, I embedded the human ES cell clumps at different densities in Matrigel. Only cell clumps embedded at high density (~1500 clumps/100 μl Matrigel) could form neuroepithelial cysts characterized by morphology (Figure 2.6 a). Cell clumps embedded at low density (~150 clumps/100 μl Matrigel) failed to achieve the integrity of pseudostratified epithelial cysts as the majority of clumps did not have a clear apical lumen and lacked a smooth basal edge (Figure 2.6 a). Interestingly, adding extrinsic FGF2 could largely rescue the formation of pseudostratified epithelial cysts at low density in Matrigel from 4±1% to 66±8% (Figures 2.6 a, b). This suggests that paracrine FGF signaling enhances epithelium integrity. The majority of the rescued pseudostratified epithelial cysts at low density supplemented with FGF2 were $PAX6^-$. It will be of great interest to examine whether other secreted factors are involved in the uniform neural identity of human ES cell-derived cysts.

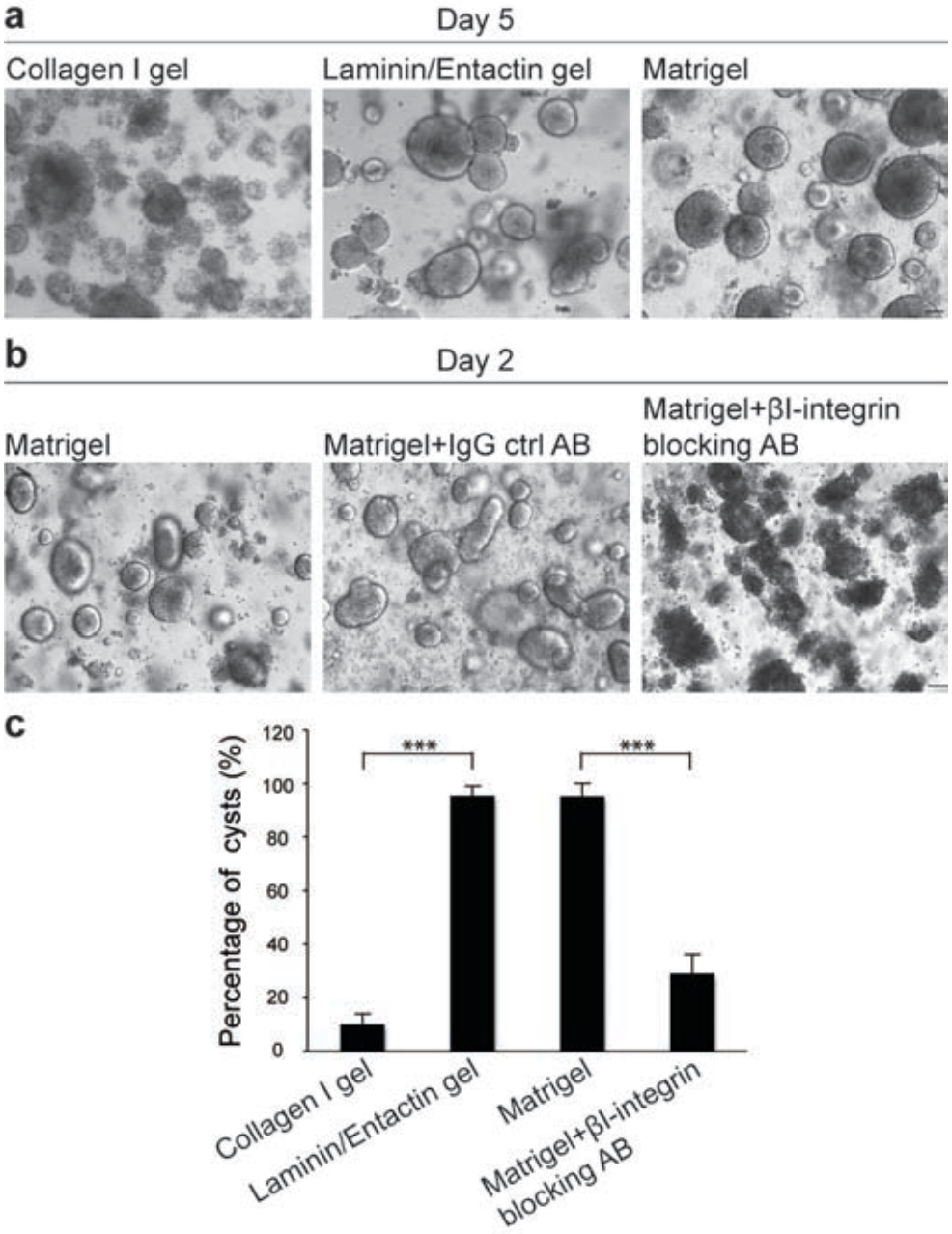

Figure 2.5 Laminin/Entactin is required for efficient cyst formation from human ES cells.

(a) Phase contrast images of human ES cell clumps growing in Collagen I gel, Laminin/Entactin gel or Matrigel. By Day 5, cell clumps failed to form cyst-like structures in Collagen I gel (left panel) but healed into single lumen contained cysts in both Laminin/Entactin gel and Matrigel. (b) Phase contrast images of human ES cell clumps growing in Matrigel with or without βI-integrin blocking antibody or IgG control antibody in the differentiation medium. At Day 2, the majority of the cell clumps failed to form cysts and stayed as unorganized clumps in the presence of βI-integrin blocking antibody (right panel), but not in the non-treated or control antibody treated samples. (c) Quantitative data for the percentage of cysts formed from human ES cell clumps at representative conditions. Ctrl: control; AB: antibody; ***: $P<0.001$. Scale bar, 50 μm.

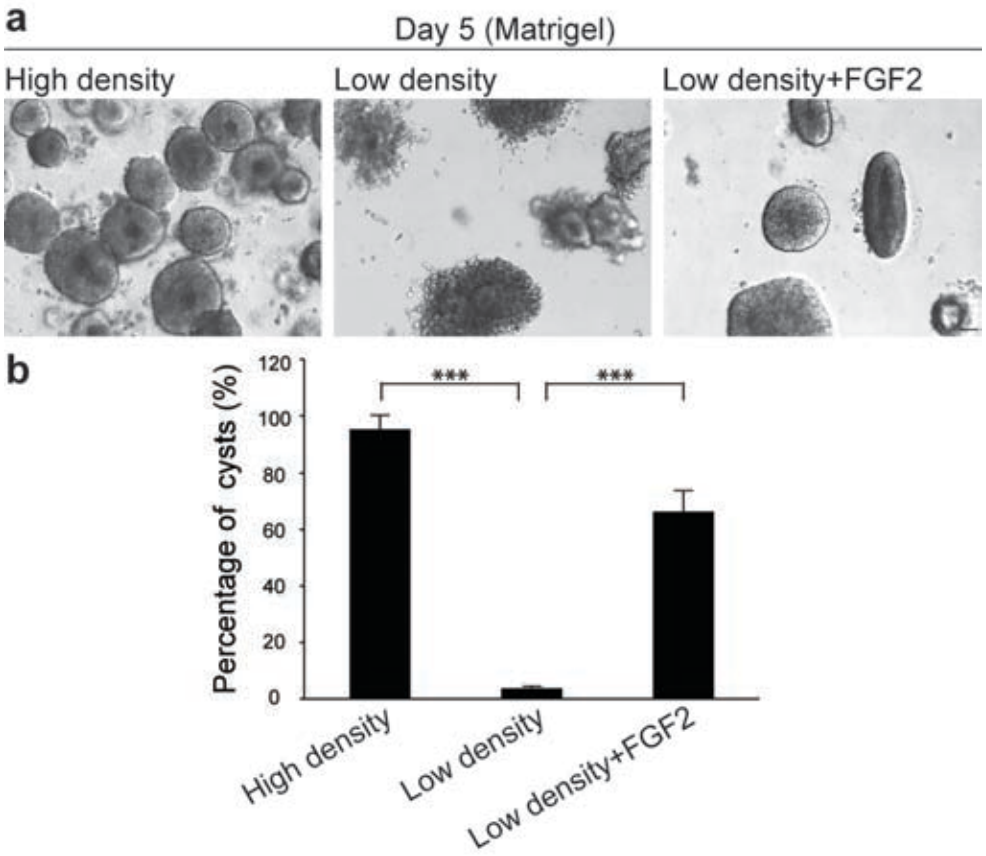

Figure 2.6 FGF signaling is required for efficient cyst formation from human ES cells.

(a) Human ES cell clumps could only form cysts with an apical lumen and smooth basal edge in Matrigel at high clump-embedding density but not at 10-fold lower density. Adding FGF2 (10 ng/ml) in the differentiation medium could rescue the formation of cysts from human ES cell clumps when embedded at low density in Matrigel (right panel). (b) Quantitative data for the percentage of cysts formed from human ES cell clumps at representative conditions. ***: $P<0.001$. Scale bar, 50 μm.

2.4 Discussion and remained questions

In summary, this work demonstrates that the application of Matrigel-based 3D epithelial cyst culture to both mouse and human pluripotent stem cells results in efficient reconstitution of neuroepithelial structure including formation of a single lumen. The generation of neuroepithelial cysts within a basement membrane setting, as described here, differs significantly from production of floating cultures such as embryoid bodies or neural aggregates. Our protocol results in uniform formation of neuroepithelial cysts each containing a single lumen. These cysts are highly organized and uniform in cell composition compared to a typical embryoid body that is a mixture of cells from three germ layers or a neural aggregate that is heterogeneous in neural cell composition and epithelial structure.

The mouse EpiS and human ES cells undergo accelerated morphogenesis and differentiation toward neuroepithelium when cultured as 3D cysts compared to other protocols(Chambers et al., 2009; Eiraku et al., 2008; Elkabetz et al., 2008). The mouse cells form $SOX1^+$ neuroepithelium within 1 day, and the human cells form $PAX6^+$ neuroepithelium within 5 days representing a two to three fold enhancement in speed of neural induction compared to previously described protocols. Interestingly, kidney epithelial cyst formation displays different kinetics depending on whether cysts are formed in Collagen I or Matrigel. MDCK cells form cysts more slowly in Collagen I using an apoptosis based mechanism to form the central lumen whereas in Matrigel epithelial architecture is achieved more rapidly in a process involving cell rearrangement rather than apoptosis(Martin-Belmonte et al., 2008). It is conceivable that the mouse EpiS and human ES cells are able to access such rapid epithelial organization programs when surrounded in three dimensions with Laminin-rich matrix, as opposed to the 2D context. I further show here that production of FGF by the differentiating cells seems to be a crucial component of efficient epithelialization. Conditioning of the local media in 2D cultures is clearly less efficient than in 3D cultures and therefore may also explain some of the discrepancies in kinetics.

While dissecting out mechanisms involved in efficient neuroepithelial cyst formation from human ES cells, I have proved that Laminin and FGF signaling are required for efficient cyst formation. Defined Laminin/Entactin at high concentration could

substitute for Matrigel to support efficient neuroepithelial cyst formation when cell clumps are embedded at high density. We further proposed a hypothesis that a 3D gel may enhance the accumulation of secreted growth factors to explain the significantly high neural induction efficiency in our neuroepithelial cyst model compared to 2D cultures. However, though extrinsic FGF2 could rescue the 3D pseudostratified epithelial cyst structure at low embedding density, these rescued cysts were $PAX6^-$ indicating their non-neural identity. There might be other secreted signalings other than paracrine FGF being responsible for the neural identity of the formed cysts. It would be interesting to set up experiments in the future such as microarray to compare the components of the conditioned media from samples at high and low clump embedding density to make the involved signalings clear.

Chapter 3

An application of human ES cell-derived neuroepithelial cyst system in retinal differentiation

Taking advantage of the high efficiency of neural induction in human ES cell-derived neuroepithelial cysts system, I further studied the regional identity of the generated neuroepithelium, and its susceptibility to cell fate determination by soluble factors.

3.1 Human ES cell-derived neuroepithelial cysts enter eyefield naturally in Matrigel

3.1.1 Regional identity of human ES cell-derived neuroepithelial cyst by RT-PCR

To check the regional identity of the human ES cell-derived neuroepithelial cysts, I did RT-PCR on a group of regional markers in central nervous system. In 2D culture, human ES cell-derived neuroectodermal cells adopt anterior neuroepithelial characteristics(Elkabetz et al., 2008; Pankratz et al., 2007). As shown in Figure 3.1, analysis of neuroepithelial cysts at different time points by RT-PCR showed a reduction of the pluripotency marker *OCT4* together with up-regulation of the neuroectodermal marker *SOX1* confirming neural induction. Consistent with an anterior phenotype, the cysts were positive for *BF-1* and *PAX2* and negative for *HOX B1* and *HOX C5*, which are more posterior markers for hindbrain and spinal cord respectively. Since expression of *BF-1* and *PAX2* suggests a characteristic possibly in the eyefield(Baumer et al., 2003; Hatini et al., 1994), I examined the expression of eyefield transcription factors (EFTFs), including *PAX6*, *RX* and *SIX3(Zuber et al., 2003)*. All three of these transcripts were up-regulated from Day 5 on. To further confirm the eyefield potential of the human neuroepithelial cysts I examined later time points for later markers of retinal differentiation. When cysts continued to be cultured in Matrigel, the RPE-specific transcription factor *MITF* started to be expressed at Day 10. The neural retina-related transcription factor *CHX10* was strongly expressed from Day 10 on, suggesting that by Day 10 the cultures represented a mixture of RPE and neural retina biased cells. Weak expression of *CRX* that is highly expressed in photoreceptor precursors was also detected from Day 10 on. Taken together, human ES cell-derived cysts formed in Matrigel naturally express eyefield progenitor genes as a population.

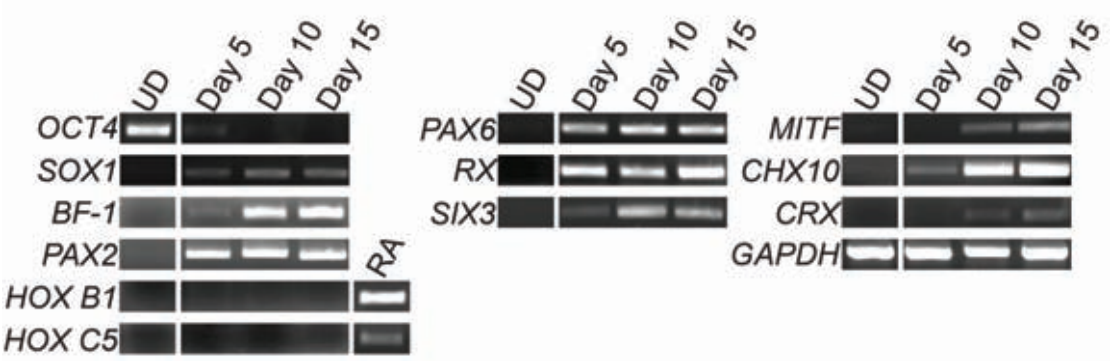

Figure 3.1 RT-PCR analyses for genes involved in regional identity.

RT-PCR analyses for genes involved in regional identity on undifferentiated human ES cells (UD) and human ES cell-derived neuroepithelial cysts at representative time points. Retinoic acid (RA) treated cysts were used as a positive control for *HOX B1* and *HOX C5*.

3.1.2 Quantitative analyses of eyefield induction in human ES cell-derived neuroepithelial cyst system by immunostaining

To quantitatively assess the efficiency of eyefield induction at the individual cell level, I immunostained the cysts for the early optic vesicle stage-related markers PAX6, RX, OTX2 and the neural retina-related marker CHX10. The specificity of the antibodies was verified on mouse embryonic cryosections (see Figure 3.2).

Almost all the human ES cell-derived cysts at Day 5 were $PAX6^+$ (99±1%) and most of them were $OTX2^+$ (97±2%) and RX^+ (92±5%). Within the positive cysts, near uniform expression of PAX6, OTX2 and RX was observed. CHX10 was rarely expressed in Day-5 cysts (Figure 3.3). At Day 15, most of the cysts maintained expression of PAX6, RX and OTX2 while many cysts became $CHX10^+$ (61±2%) (Figure 3.3).

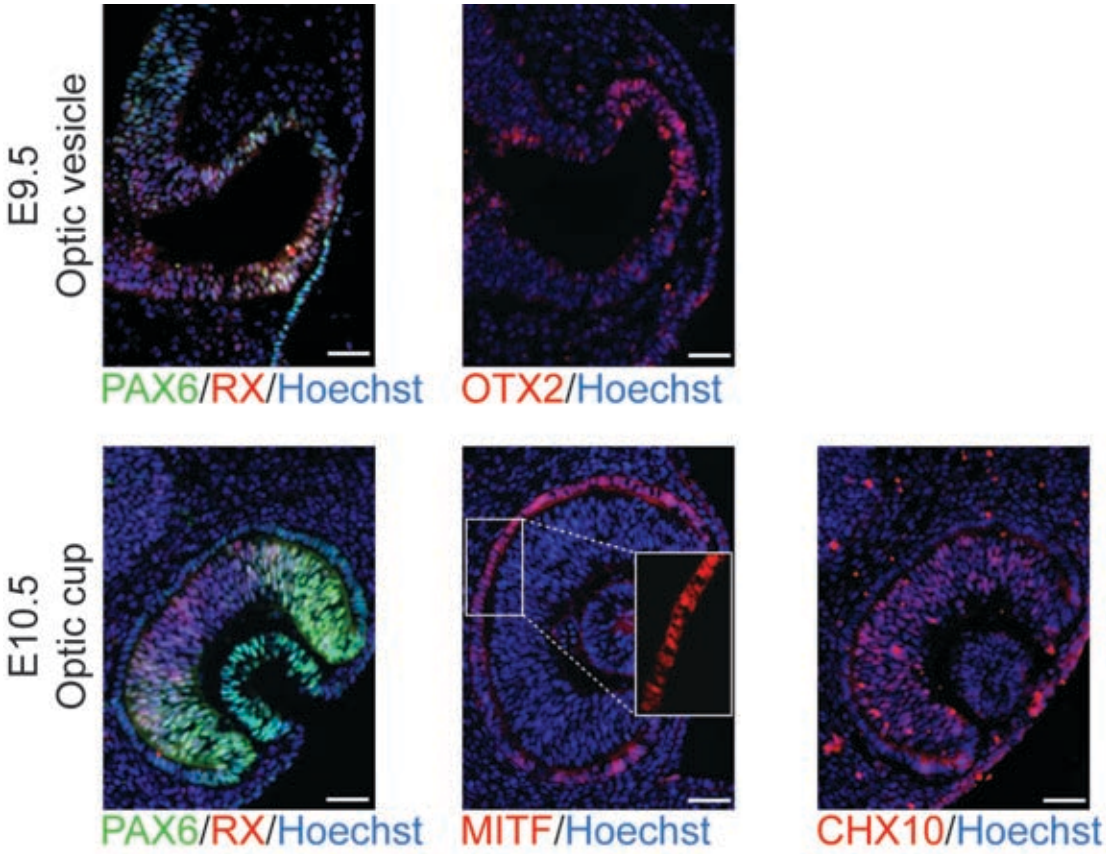

Figure 3.2 Specificity of antibodies on embryonic mouse sections in the eyefield.

The antibodies used for immunostaining were tested on mouse embryonic sections in the eyefield at representative stages. Inset: higher magnification view confirming the nuclear staining of MITF. Nuclei were counterstained with Hoechst. Scale bar, 50 μm.

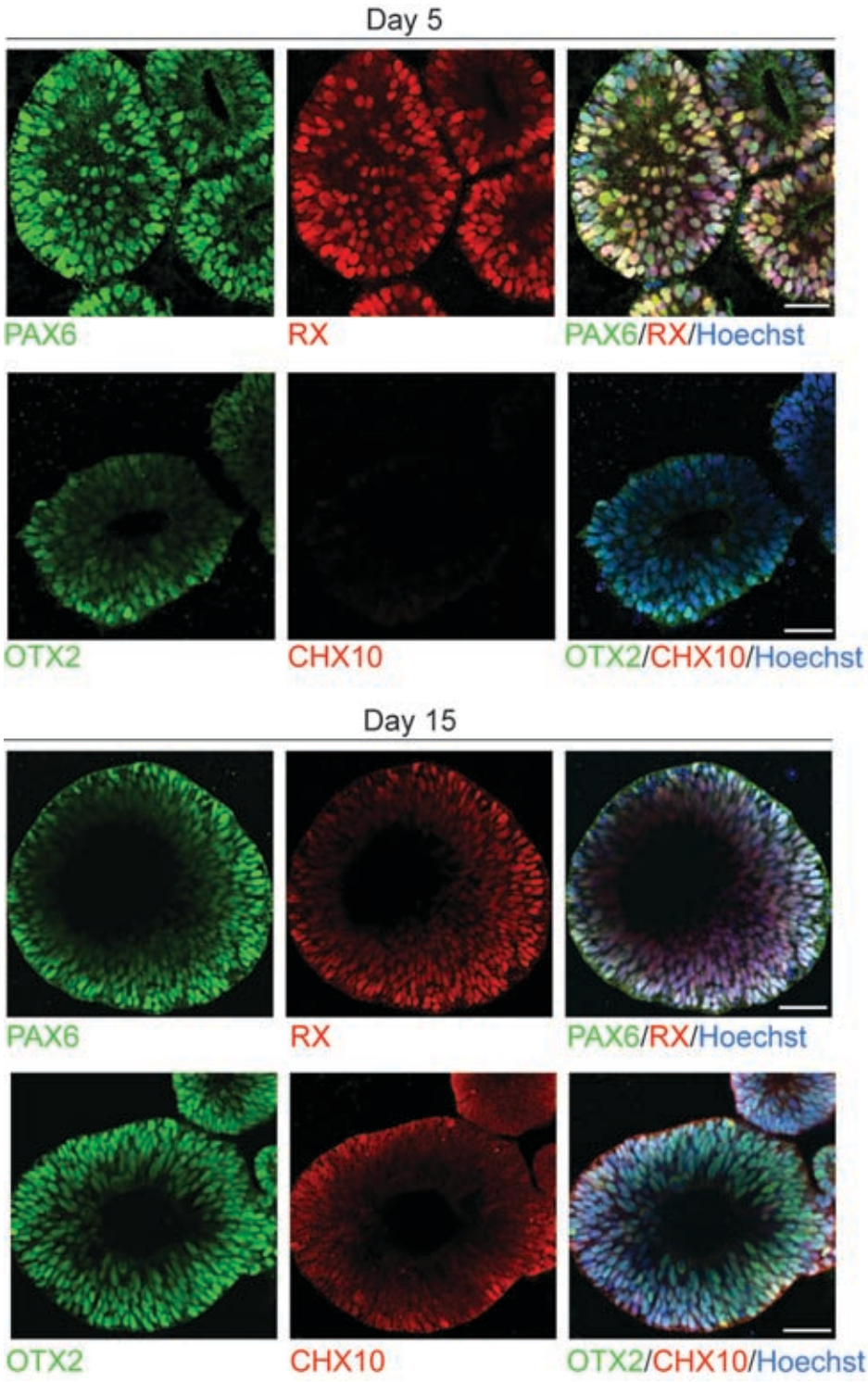

Figure 3.3 Human ES cell-derived neuroepithelial cysts enter and maintain retinal identity.

Immunocytochemical analysis of human ES cell-derived cysts at Day 5 and Day 15 as indicated. Day-5 cysts were positive for PAX6 (green), RX (red) and OTX2 (green) but few $CHX10^{+}$ cells were detected at Day 5, indicating that cells achieved an optic vesicle identity. $CHX10^{+}$ (red) cells were detected at Day 15. Nuclei were counterstained with Hoechst. Scale bar, 50 μm.

To confirm the results of the antibody staining, I performed *in situ* hybridization to detect the corresponding messenger RNA on cryosectioned cysts (Figure 3.4). These cryosectioned cysts showed strong signals for *PAX6* and *RX* especially apically (Figure 3.4 a) indicating that the stronger basal signal in the wholemount immunofluorescence of large cysts (Figure 3.3) was due to the hindered penetrance of the antibodies into the center of the cyst. Induction of eyefield identity was also observed in high concentration of Laminin/Entactin gel with similar efficiency. Though high concentration of Laminin/Entactin gel could substitute for Matrigel in generating eyefield neuroepithelial cysts from human ES cells, further experiments were mostly done in Matrigel unless specified, due to the high cost of Laminin/Entactin gel. We conclude from these results that the vast majority of human ES cell-derived cysts at Day 5 acquire an optic vesicle cell phenotype.

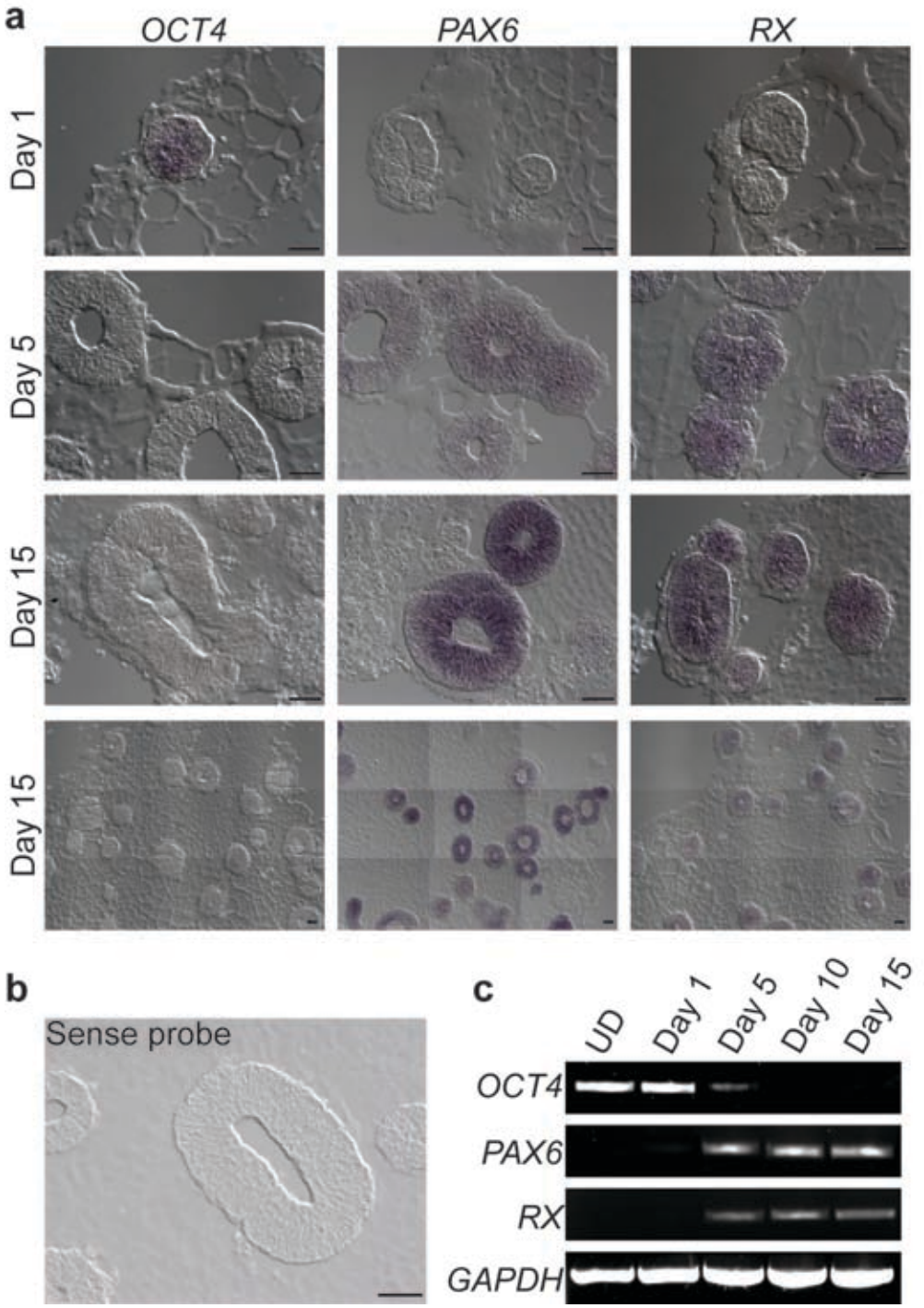

Figure 3.4 Expression of OCT4, PAX6 and RX at the RNA level in human ES cell-derived neuroepithelial cysts at representative time points.

(a) *In situ* hybridization of *OCT4*, *PAX6* and *RX*. Day-1 cryosectioned cysts were positive for *OCT4* but negative for *PAX6* and *RX*. Day-5 and Day-15 cryosectioned cysts were positive for *PAX6* and *RX* but negative for *OCT4*. The bottom row showed an overview of *OCT4*, *PAX6* and *RX* expression on Day-15 cysts in mosaic images. (b) *In situ* hybridization using sense probes as negative controls on cryosectioned cysts. (c) RT-PCR analyses confirmed the RNA expression of *OCT4*, *PAX6* and *RX* at corresponding time points. Scale bar, 50 μm.

3.2 Differentiation of human eyefield cysts into neural retina tissue

Embryological studies have shown that cells of the early eyefield have the potential to form either neural retina or RPE, depending on the presence of different soluble factors(Fuhrmann, 2010). Given the high efficiency with which we could induce optic vesicle stage cells, we sought to test the susceptibility of the generated neuroepithelium to cell fate determination and thus try to further differentiate them toward neural retina and RPE.

I first examined whether the Day-5 optic vesicle cells could be differentiated into neural retina under strictly defined conditions by plating cysts onto transwell filters and further culturing in neural induction medium N2B27 (see Figure 3.5), since Matrigel is a rich basement membrane containing many growth factors.

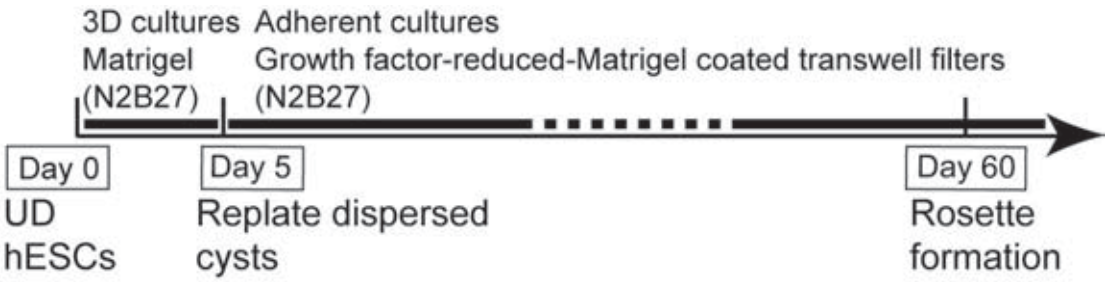

Figure 3.5 Schematic of protocol on directed neural retina differentiation from human ES cell-derived neuroepithelial cysts.

UD: undifferentiated.

To analyze the cell population during neural retina differentiation, I chose a group of neural retina-related genes CRX, CHX10 and PAX6 for immunostaining. CRX, as a photoreceptor precursor marker, has high sequence similarity with OTX2. Commercially available CRX antibodies often cross-react with OTX2. We thus made

our own CRX antibody (see more details in Chapter 4 Materials and methods). The specificity of the antibodies were verified on mouse embryonic cryosections (Figure 3.6). CRX^+ cells mostly located in the outer nuclear layer labeling photoreceptor precursors. A few CRX^+ cells in the outer part of inner nuclear layer might either differentiate into bipolar cells or migrate into the outer nuclear layer and become photoreceptor cells. The expression pattern of CRX on cryosectioned P7 mouse eye showed in Figure 3.5 using our home-made CRX antibody was consistent with previous report(Furukawa et al., 1997). CHX10 expression was restricted to bipolar cells in the inner nuclear layer during retinal development while PAX6 antibody labeled mostly amacrine, horizontal and ganglion cells.

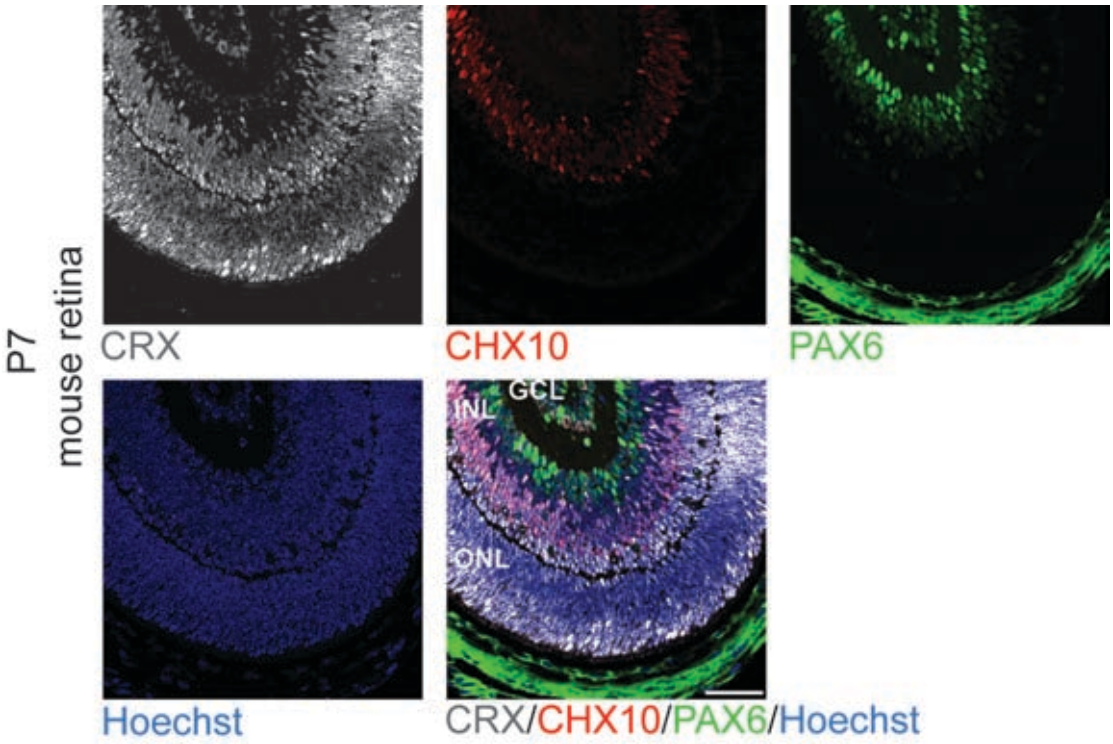

Figure 3.6 Specificity of antibodies on P7 mouse retina.

GCL: ganglion cell layer. INL: inner nuclear layer. ONL: outer nuclear layer. Nuclei were counterstained with Hoechst. Scale bar, 50 μm.

These conditions described in Figure 3.5 resulted in cultures where >99% of cells were $CHX10^+$ and/or $PAX6^+$ by 20 days (Figure 4B). By 60 days, cells had self-organized into stratified rosette-like structures with a high percentage of CRX^+ cells surrounded by $CHX10^+PAX6^{+weak}$ and $CHX10^-PAX6^{+strong}$ cells (Figure 3.7). This stratified structure was very similar to the layered structure seen in the intact mouse retina (Figure 3.6).

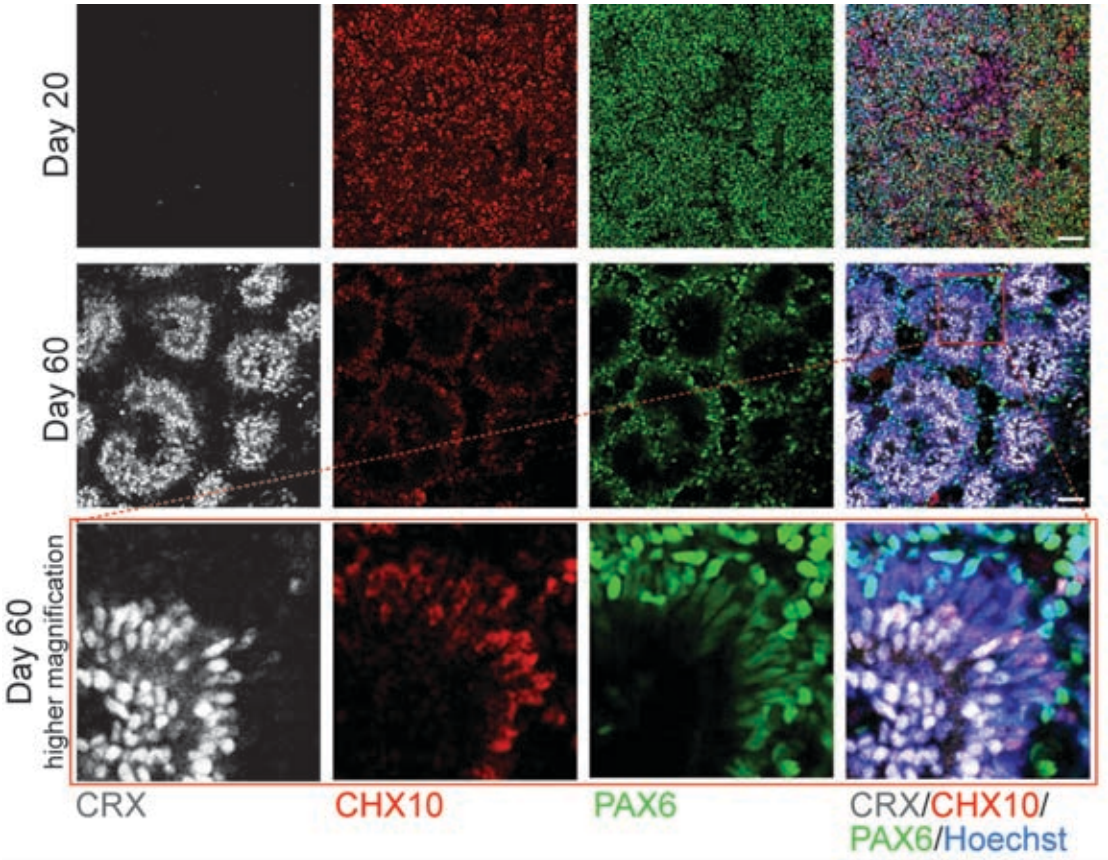

Figure 3.7 Directed differentiation of human ES cell-derived neuroepithelial cysts to neural retina cells using transwell filters.

Immunostaining of CRX (white), CHX10 (red) and PAX6 (green) at Day 20 (upper row) and Day 60 (lower row) during neural retina differentiation. The expression of CRX was up-regulated gradually. By Day 60, CRX-positive cells were surrounded by CHX10 and/or PAX6-positive cells in a rosette-like structure. Inset: higher magnification view. Nuclei were counterstained with Hoechst. Scale bars, 50 μm.

3.3 Differentiation of human eyefield cysts into RPE cells

3.3.1 Generation of pigmented cells from human eyefield cysts on transwell filters

To check whether human eyefield cysts were limited to neural retinal differentiation, I next characterized RPE differentiation. As with neural retina induction, I dispersed Day-5 cysts and plated them onto transwell filters coated with growth factor-reduced-Matrigel to obtain polarized epithelial cells but the culture medium was changed from neural induction medium (N2B27) to a standard RPE-supporting medium containing knockout serum replacement (Figure 3.8).

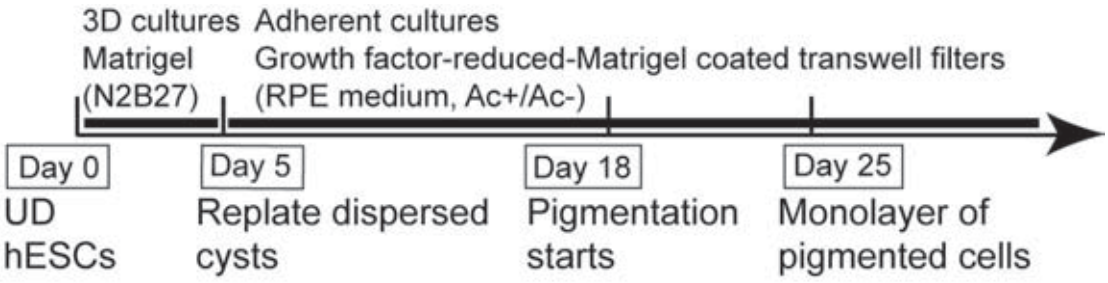

Figure 3.8 Schematic of protocol on directed neural retina differentiation from human ES cell-derived neuroepithelial cysts.

UD: undifferentiated. Ac+/Ac-: with or without Activin A.

In the presence of 100 ng/ml Activin A, a known inducer of RPE fate(Fuhrmann et al., 2000; Idelson et al., 2009; Meyer et al., 2011), I observed the appearance of pigmented RPE-like cells starting around Day 18 with the characteristic polygonal shape emerging starting Day 25. By Day 30, 96±1% cells were pigmented, whereas in the absence of Activin A only isolated pigmented colonies appeared (Figure 3.9).

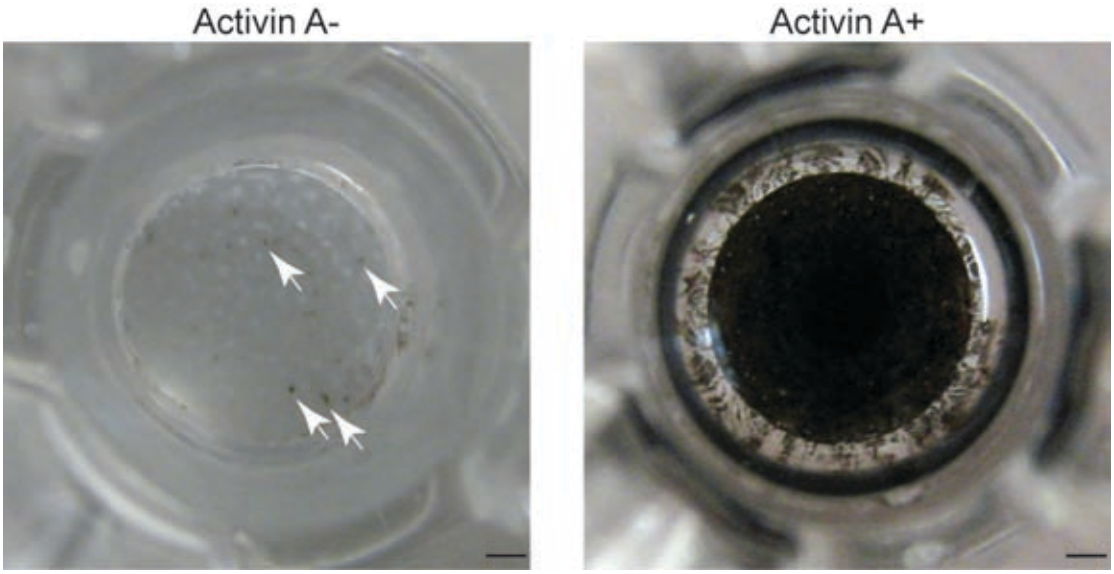

Figure 3.9 Directed differentiation of human ES cell-derived neuroepithelial cysts to pigmented cells using transwell filters.

Top view of transwell filters at 30 days of culture showing the appearance of a pigmented cell sheet in the presence of Activin A (100 ng/ml) but not in its absence. Arrows ( ) point to a few pigmented foci in the non-Activin A treated sample. Scale bars, 1 mm.

Interestingly, Activin A-dependent RPE induction was highly sensitive to the initial cell seeding density onto the transwell filters (Figure 3.10). Taking human ES cell line H9 as an example, when the cell seeding density was too low ($\leq 1x10^5$ cells/0.3 cm^2), attached cells could not survive during Activin A (100 ng/ml) treatment. Severe cell death was observed under low cell seeding density condition. However, when the cell seeding density was too high ($\geq 4x10^5$ cells/0.3 cm^2), the percentage of pigmented cells decreased significantly after Activin A (100 ng/ml) treatment. The best seeding density window should be adjusted for each cell line.

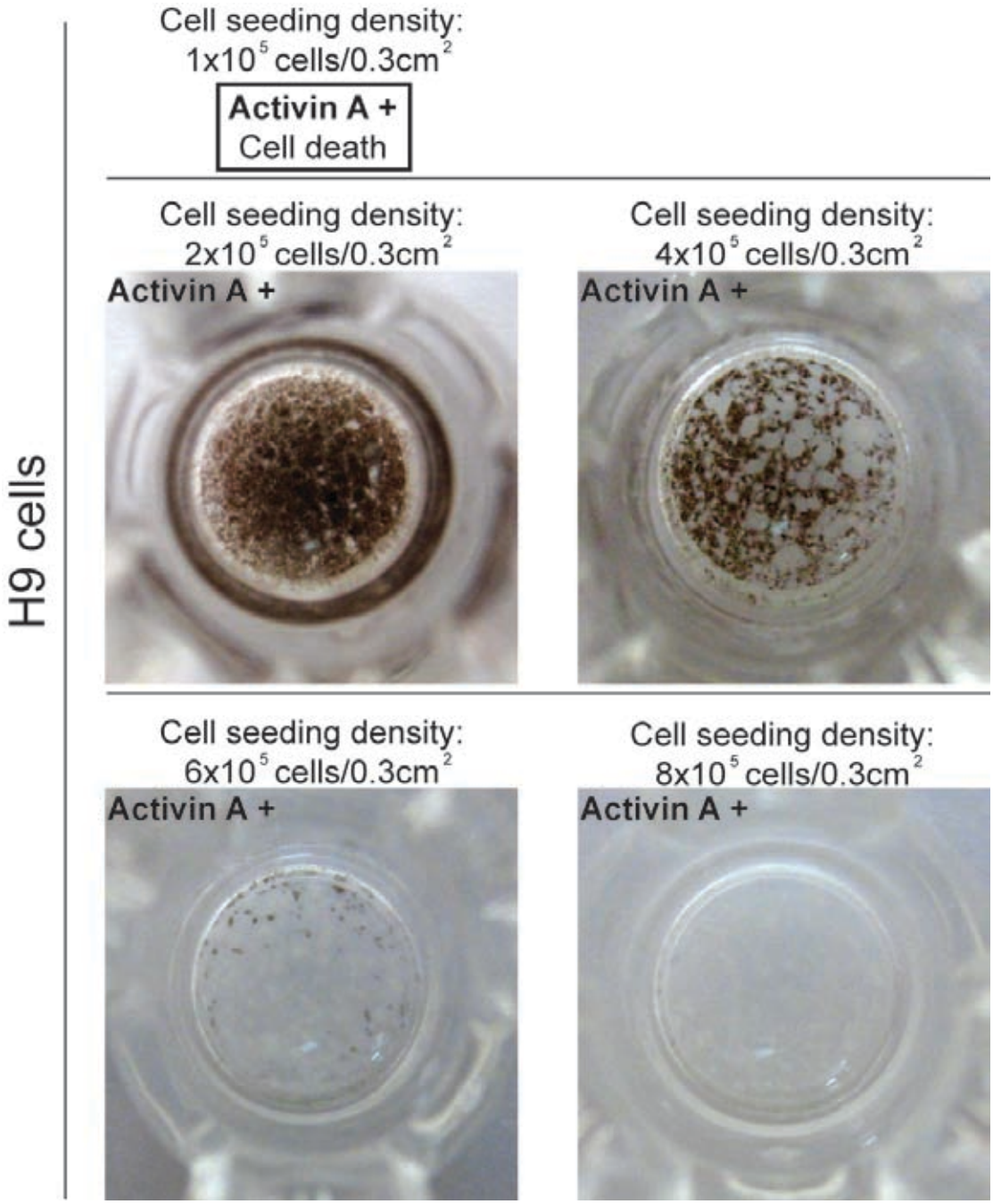

Figure 3.10 RPE-like cell determination from human ES cell H9-derived neuroepithelial cysts was dependent on cell seeding density.

Top view of transwell filters showing the appearance of pigmented cells derived from H9 cells at Day 25 at different seeding densities in the presence Activin A (100 ng/ml). Too high or too low cell seeding density failed to induce the formation of a pigmented cell sheet. Scale bar: 1 mm.

The bulk of my analysis on human ES cells was performed on the human ES cell line H9 but I confirmed that my human ES cells-neuroepithelial cyst-pigmented cell protocol worked efficiently on different human pluripotent cell lines. In the H9 work, the addition of Activin A significantly enhanced the appearance of pigmented cells (Figure 3.9) and efficient RPE induction was highly sensitive to cell seeding density in the presence of Activin A (Figure 3.10). When using the H1 cell line, the RPE differentiation efficiency and timeline was very similar compared to that for H9 but exogenous Activin A was not required for pigmented cell formation. However, the pharmacological Activin/TGF-β inhibitor SB 431542 completely blocked pigmentation in the H1 cells, indicating Activin-like signaling is indeed required and apparently made endogenously during RPE-like cell differentiation from H1 cells (Figure 3.11).

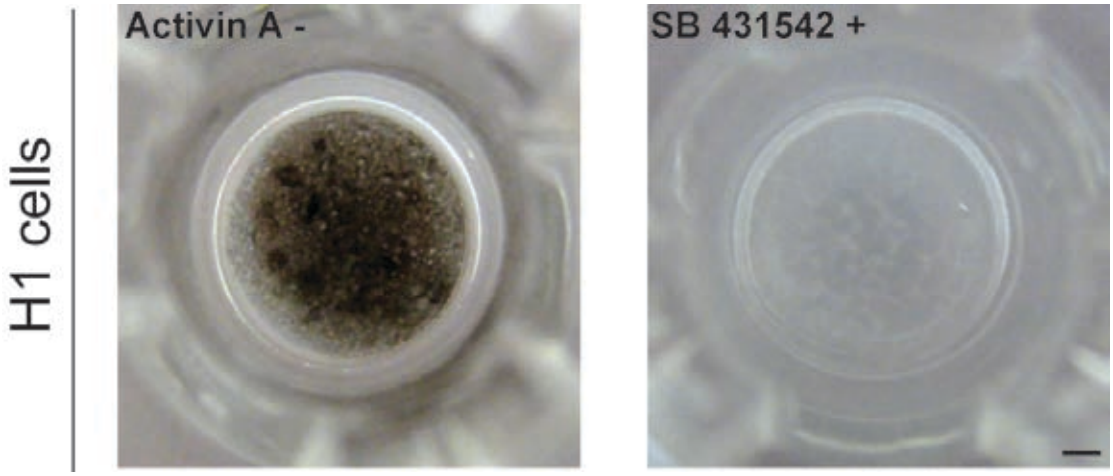

Figure 3.11 RPE-like cell determination from human ES cell H1-derived neuroepithelial cysts was dependent on TGF-β signaling.

Differentiation of H1 cells to RPE does not require exogenous Activin A but does depend on TGF-β/Activin-related signaling. Top view of transwell filters showing the appearance of pigmented cells derived from H1 cells at Day 25 in the presence or absence of SB 431542 (8 μM). The TGF-β inhibitor SB 431542 completely blocked the pigmentation of cells. Scale bar, 1 mm.

I also determined if the method was effective on the human iPS cell line O27-08. The timescale of cyst formation and RPE-like cell differentiation were indistinguishable from those of human ES cells (Figure 3.12 a, b). During differentiation, immunostaining revealed that the human iPS cell-derived cysts were also positive for early eyefield progenitor markers PAX6, RX and OTX2 with the tight junction marker ZO-1 toward the apical side (Figure 3.12 c). However, we found PAX6 expression in O27-08 cell-derived cysts was weaker compared to that in human ES cell-derived cysts. This coincides with previous reports in which considerable variation was found in the ability of different iPS cell lines to differentiate into $PAX6^{+}$ neuroectodermal cells(Hu et al., 2010a; Meyer et al., 2009). Although the percentage of pigmented cells differentiated from O27-08 cells (Figure 3.12) was lower compared to the H9 and H1 human ES cells, we obtained a relatively high percentage of RPE cells in the 30-day timescale (48±6% pigmented cells), still representing a significant improvement to other RPE protocols used on ES cells(Buchholz et al., 2009; Idelson et al., 2009; Klimanskaya et al., 2004; Meyer et al., 2009; Osakada et al., 2008; Vugler et al., 2008). It is likely that boosting PAX6 induction by other exogenous factors, or using iPS cell lines biased toward RPE formation(Hu et al., 2010b) would rescue this lower efficiency.

Collectively, the current approach of human pluripotent stem cell-neuroepithelial cyst-RPE-like cell efficiently directs human pluripotent stem cells toward pigmented cells that have morphological properties similar to native RPE cells and form a confluent pigmented cell layer without the need for clonal expansion.

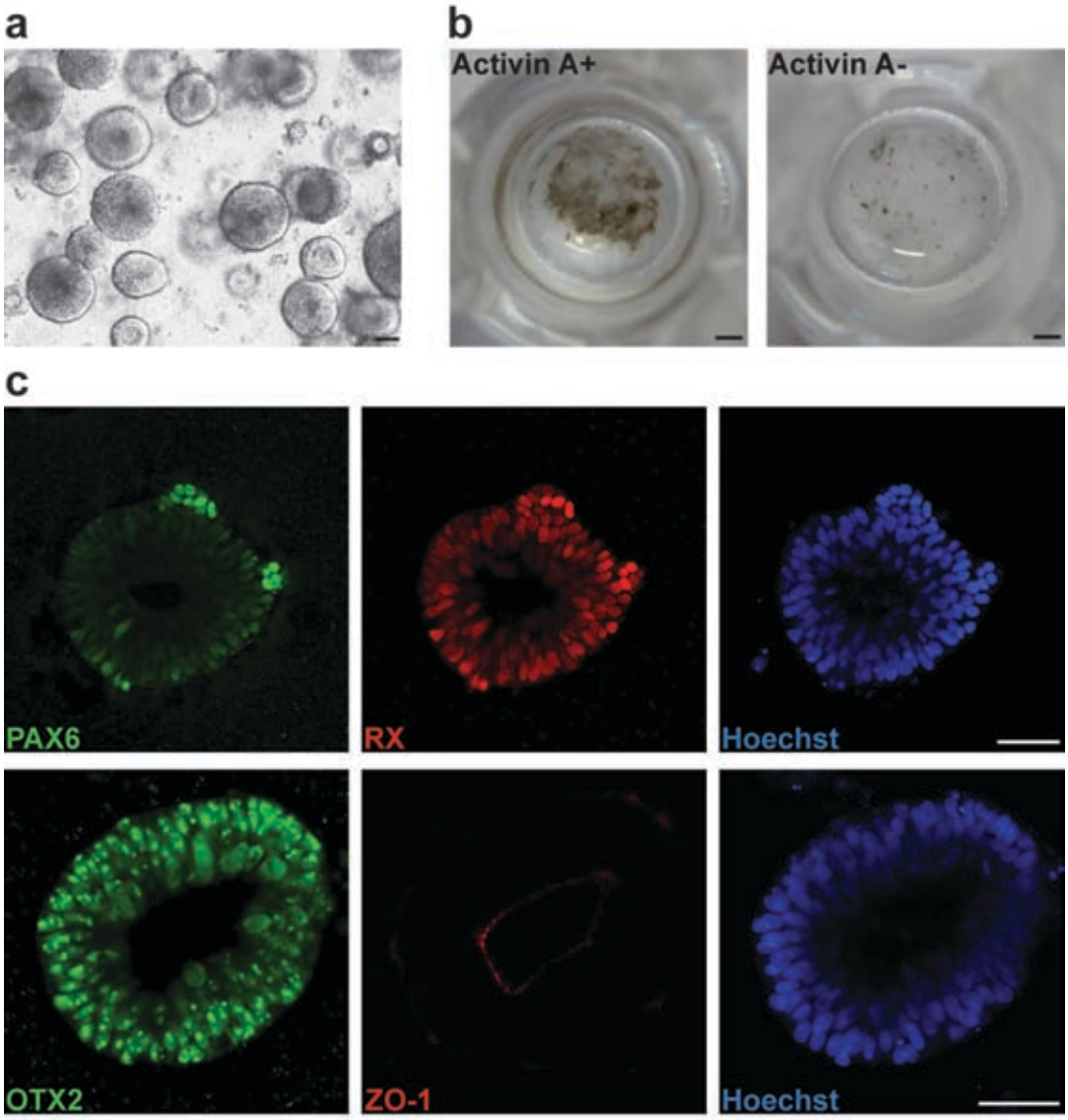

Figure 3.12 Differentiation of RPE-like cells from human iPS cells.

(a) A phase contrast image of human iPS cell-derived cysts at Day 5. (b) Top view of transwell filters showing the appearance of pigmented cells derived from human iPS cells at Day 30 in the presence or absence of Activin A (100 ng/ml). (c) Human iPS cell-derived cysts were positive for PAX6 (upper row, green), RX (upper row, red) and OTX2 (lower row, green) at Day 5. The expression level of Pax6 was low. ZO-1 (lower row, red) was expressed toward the apical side of the cysts indicating polarized epithelial phenotype. Nuclei were counterstained with Hoechst. Scale bars, 1 mm (b), 50 μm (others).

3.3.2 Characterization of human ES-cell derived RPE-like cells

To characterize the pigmented cells generated from human eyefield cysts, I did a variety of molecular, ultrastructural and functional assays. I first performed a time-course analysis of some key features during RPE development to monitor the differentiation process. PAX6 expression remained stable throughout while the expression of the RPE-specific marker MITF initiated in the majority of the cells by 22 days (Figure 3.13).

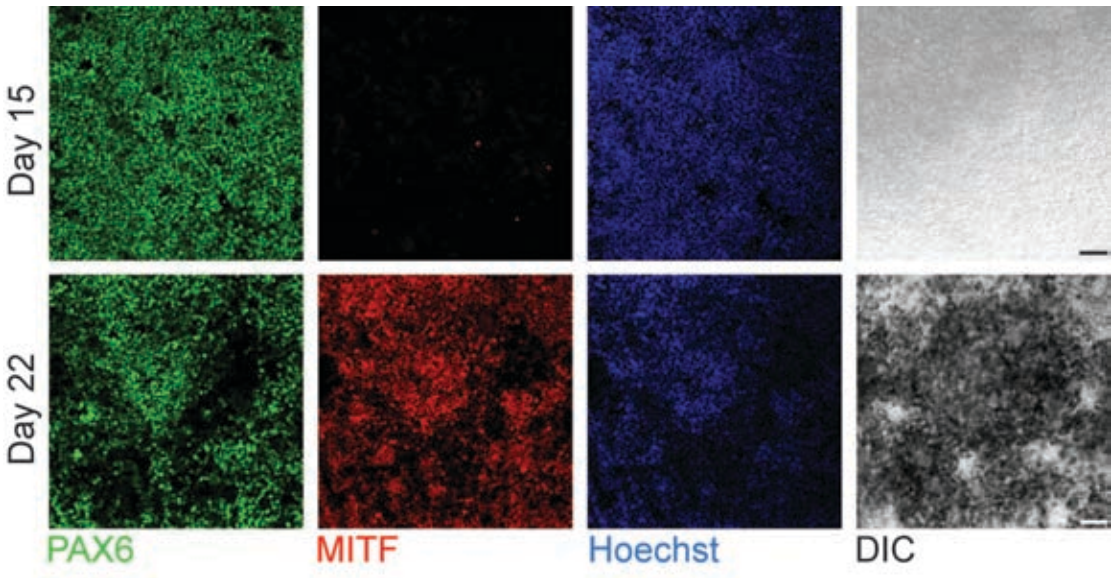

Figure 3.13 Time course analysis during RPE-like cell differentiation.

Immunostaining of PAX6 (green) and MITF (red) at Day 15 (upper row) and Day 22 (lower row) during RPE differentiation. Expression of PAX6 stayed stable, while MITF was up-regulated by day 22. Nuclei were counterstained with Hoechst. Scale bars, 1 mm (D), 50 μm (others).

In the RPE-like cell cultures, robust ZO-1 immunofluorescence (Figure 3.14 a) indicated that the cultures formed a tight epithelial barrier. Ultrastructural analysis at Day 50 confirmed the presence of tight junctions and desmosomes and of abundant melanin granules enriched toward the apical surface that displayed the characteristic dome shape and microvilli (Figure 3.14 b-d). To functionally test the epithelial barrier function, I measured the transepithelial resistance (TER) that gradually increased to a TER of 313±4 $\Omega \cdot cm^{-2}$ at Day 50 (Figure 3.14 e). This value is within the upper range of TER measured from cultured human fetal RPE (150 and 330 $\Omega \cdot cm^{-2}$)(Frambach et al., 1990; la Cour et al., 1994), suggesting that the epithelial barrier function has been established.

To further characterize RPE differentiation, I immunostained for the mature RPE cell markers RPE65 and BESTROPHIN at Day 40, which yielded strong signal localized to the basal side consistent with differentiated RPE (Figure 3.15 a). Finally, I confirmed that the proliferating RPE progenitor cells exited the cell cycle over time based on 5-ethynyl-2'-deoxyuridine (EdU) uptake at representative time points. As shown in Figure 3.15 b, the vast majority of pigmented cells were negative for EdU by Day 30.

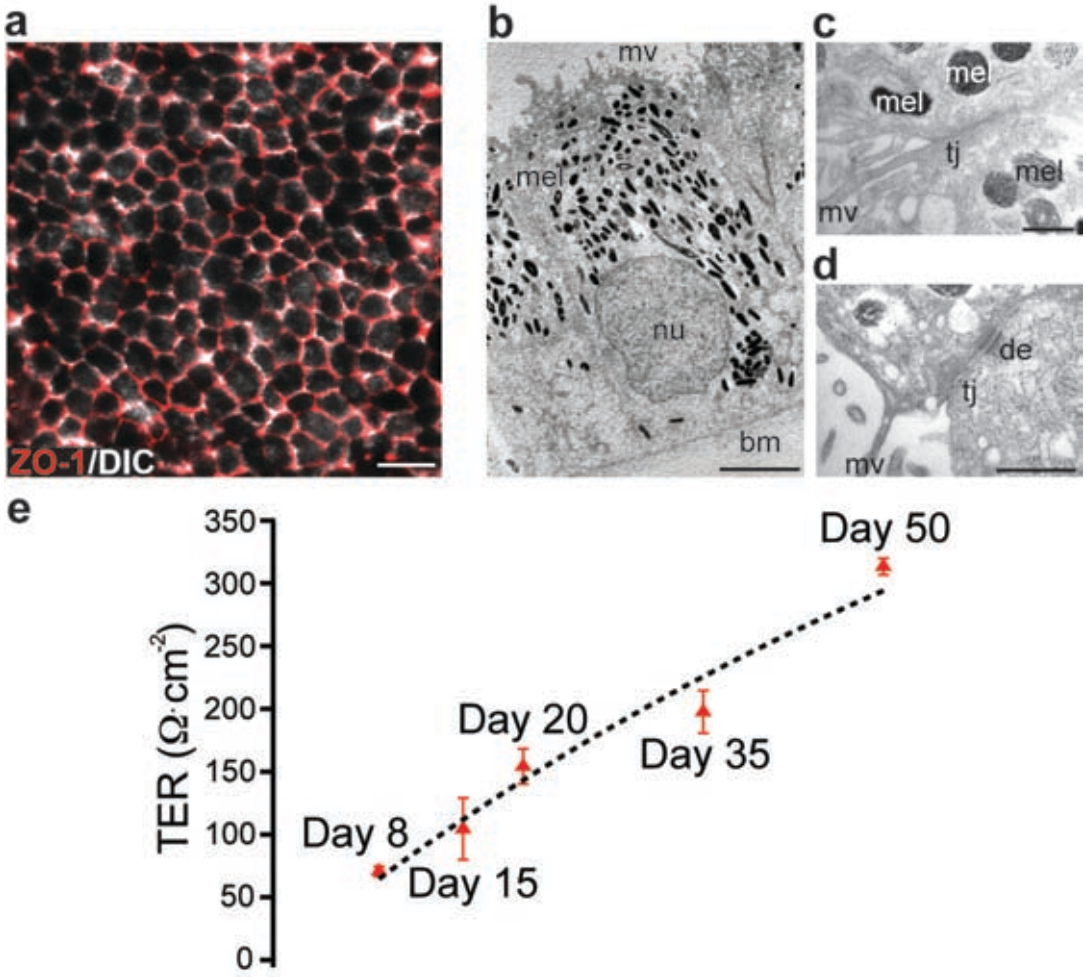

Figure 3.14 The human ES cell-derived RPE-like cell cultures formed a tight epithelial barrier.

(a) Immunostaining of ZO-1 (red) on human ES cell-derived RPE-like cells at Day 30 indicated the presence of tight junctions. Pigmented cells displayed polygonal shape. (b-d) Electron microscopic analyses of human ES cell-derived RPE-like cells at Day 50. Human ES cell-derived RPE-like cells had abundant apical microvilli (mv), melanin granules (mel) in the apical half and the nucleus (nu) in their basal half. A basement membrane (bm) was visible. Tight junctions (tj) and desmosomes (de) could be found. (e) The transepithelial resistance (TER) of human ES cell-derived RPE-like progenitors/cells increased during differentiation. Scale bars, 20 μm (a), 5 μm (b), 500 nm (c, d).

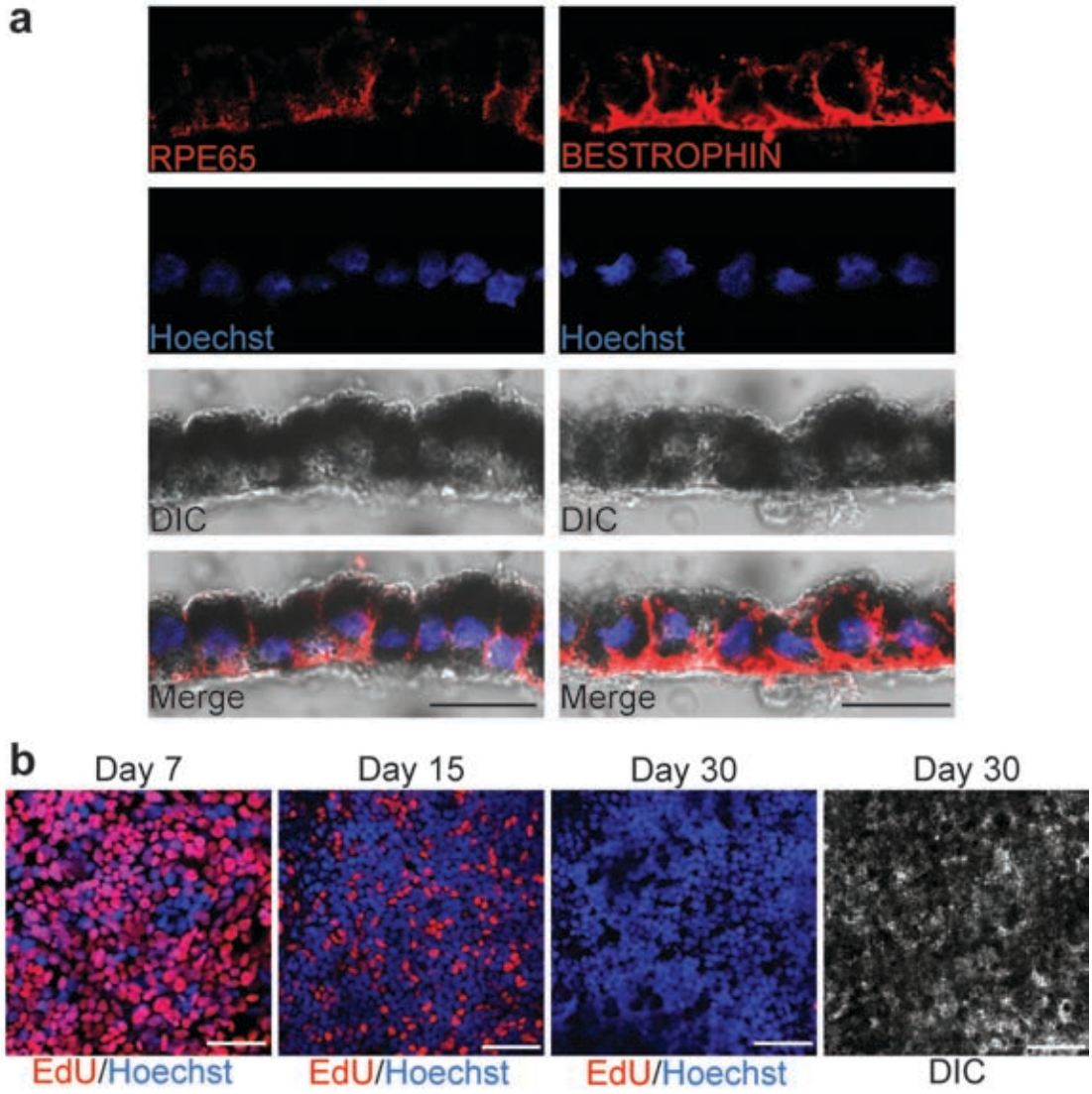

Figure 3.15 Human ES cell-derived pigmented cells showed RPE cell characteristics.

(a) Cross-sections through the pigmented cell sheet immunostained for RPE65 and BESTROPHIN. Human ES cell-derived RPE-like cells at Day 40 expressed mature RPE cell markers RPE65 and BESTROPHIN mainly in the basal side of the cells. (b) Human ES cell-derived RPE-like cells exited the cell cycle by Day 30 as demonstrated by RPE-like cultures pulse labeled with EdU at Day 7, 15 and 30. EdU incorporation by proliferating cells was observed at Day 7 and 15, but rarely observed at Day 30. Nuclei were counterstained with Hoechst. Scale bars, 20 μm (a), 50 μm (b).

One of the most important functions of RPE cells *in vivo* is phagocytosis of shed photoreceptor outer segments to support the daily renewal process of photoreceptor cells(Strauss, 2005). To analyze whether the human ES cell-derived RPE cells phagocytose shed outer segment disks, I endeavored to recapitulate the *in vivo* photoreceptor/RPE interaction by co-culturing the human ES cell-derived RPE cells with neural retinal explants from transgenic mice expressing human RHODOPSIN-GFP(Chan et al., 2004) (Figure 3.16), similar to a previous co-culture system(Carr et al., 2009). I prefer this system to the use of purified outer segment or latex bead incubation assays where it can be difficult to distinguish truly endocytosed disks from material adherent to the surface.

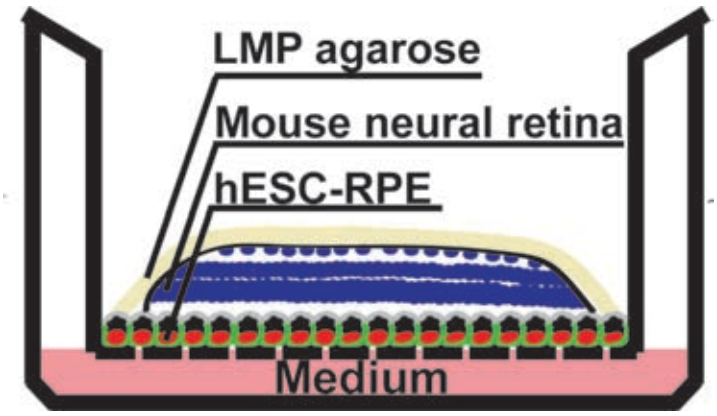

Figure 3.16 Schema of the *in vitro* co-culture model of human ES cell-derived RPE cells and mouse retinal explants to assess phagocytosis.

LMP: low melting point.

After 24 hours of co-culture, the human ES cell-derived RPE-like cells were directly juxtaposed with the mouse retina cells (Figure 3.17 a). Immunofluorescence to specifically detect human nuclei in the pigmented cell layer excluded the possibility of contamination from mouse RPE cells (Figure 3.17 b). Abundant GFP^+ outer segment structures were observed in the pigmented cells (Figure 3.17 b, see also Movie 3.1 in the attached DVD). Immunostaining of the co-cultures to detect the early endosome marker EEA1 specifically in human cells, showed EEA1 signal surrounding the GFP^+ particles, confirming that outer segments had been phagocytosed by the RPE cells (Figure 3.17 c). Taken together, our results indicate that the pigmented cells, which are directly differentiated, with no selection, from human neuroepithelial cysts, efficiently form functional RPE.

3.3.3 Trials to pattern eyefield cysts in 3D

To recapitulate the organogenesis of retina *in vitro*, I tried to further differentiate human eyefield cysts in Matrigel. Human ES cell-derived Day-5 optic vesicle stage cysts were taken out of Matrigel and re-embedded in fresh Matrigel at different densities. After 40 days of culture in N2B27 medium, no self-organized invagination was observed under light microscope. The immunostaining of CRX, the photoreceptor precursor marker, on cryosectioned long-term differentiated cysts only showed a few positive cells randomly localized in the cysts. Some CRX^+ cells were adjacent to the lumen while some were at the edge of the cysts (Figure 3.18). Some extrinsic triggers might be missing to induce the invagination and lamination process in this natural differentiation system. I therefore further co-cultured Day-5 optic vesicle stage cysts with embryonic chick lens, which plays a vital role during eye morphogenesis(Chow and Lang, 2001; Fuhrmann, 2010; Martinez-Morales et al., 2004b). When co-cultured with chick lens in Matrigel for 2 weeks, no distinct morphological changes of eyefield cysts were observed. Recent study by Sasai group(Eiraku et al., 2011) indicated that the invagination of the neural retina could occur even without forces from external structures and the morphogenesis includes multiple steps controlled in a history-dependent fashion at least in their *in vitro* mouse ES cell differentiation model. One possibility of failure to generate patterned retina layer from highly pure human optic vesicle stage cysts is that the differentiation timeline is too short to trigger morphologic changes in human system based on the

long timeline of human development. Or Matrigel that I used to support further 3D differentiation is too rich in growth factor signalings which block the default cellular organization. It would be interesting to try more neutral gels such as Collagen I or Laminin gel instead of Matrigel or suspension culture system to support further 3D differentiation of eyefield cysts for a longer term.

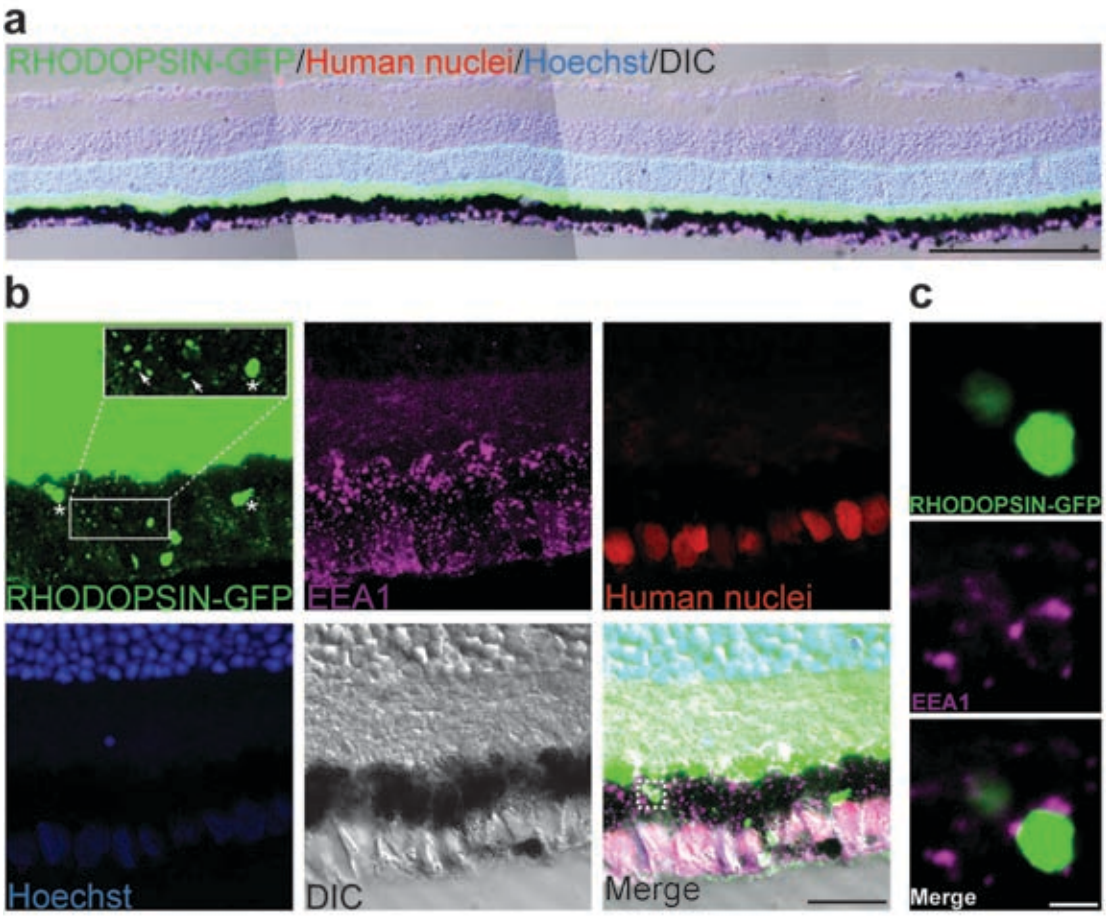

Figure 3.17 Co-culture of human ES cell-derived RPE cells and mouse retinal explants (RHODOPSIN-GFP fusion construct transgenic mice) *in vitro* to assess phagocytosis.

(a) A merged RHODOPSIN-GFP (green), human nuclei (red), Hoechst (blue) and DIC image in the co-culture model. Human ES cell-derived RPE-like cells formed a contiguous tissue sheet with the mouse retinal explant. (b) Immunocytochemical analyses on cross-sections of co-cultured human ES cell-derived RPE-like cells and mouse retinal explants. Fluorescence images represented the maximum intensity projection of serial confocal images through z-axis. Pigmented layer cells were positive for antibody staining against human nuclei (red). Stars (*) or arrows (➤) pointed to bigger or smaller pieces of GFP^+ photoreceptor outer segments (green) found within human ES cell-derived RPE-like cells. Signal for the early endosome membrane marker EEA1 using a human-specific antibody (magenta) was visible in the pigmented layer associated with phagocytosed GFP^+ outer segments. Inset in Rhodopsin-GFP channel: higher magnification view of phagocytosed outer segments. (c) A high-magnification image of dashed box in the merge channel of panel (b) showed that the EEA1 signal surrounded the GFP^+ particles. Nuclei were counterstained with Hoechst. Scale bars, 200 μm (a), 20 μm (b), 2 μm (c).

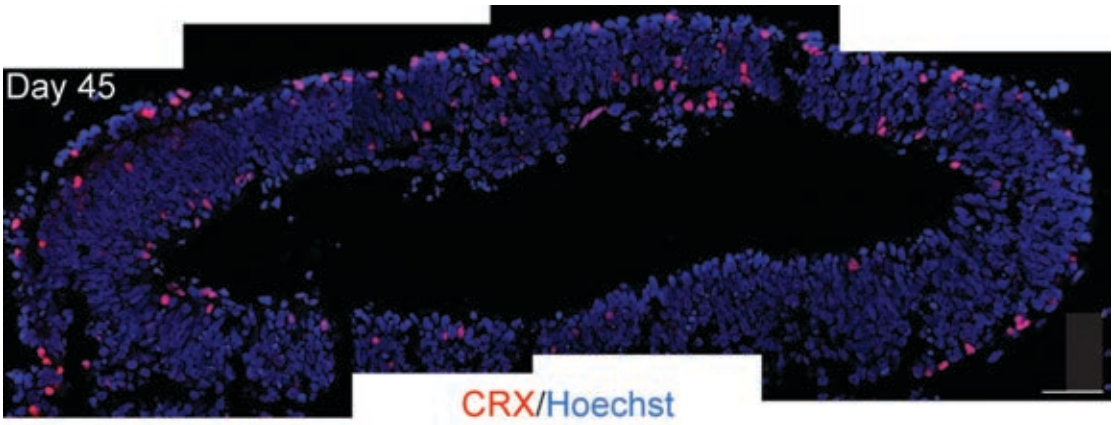

Figure 3.18 Immunostaining of CRX on cryosectioned human cysts in long-term 3D culture.

Nuclei were counterstained with Hoechst. Scale bar, 50 μm.

3.4 Discussion and remained questions

This work shows an unprecedentedly high efficiency and speed of human ES cell differentiation towards eyefield. The three-dimensional matrix conditions uniformly promoted neuroepithelial cyst formation with optic vesicle identity in 5 days, a significant acceleration from all protocols published to date(Buchholz et al., 2009; Carr et al., 2009; Hu et al., 2010b; Idelson et al., 2009; Klimanskaya et al., 2004; Lamba et al., 2006; Meyer et al., 2011; Meyer et al., 2009; Osakada et al., 2008; Vugler et al., 2008). Transferring these cells into two-dimensional epithelial cell culture conditions promoted neural retina tissue or RPE formation in high yield under different defined conditions. Remarkably, without any sorting, more than 95% RPE cells were generated from human ES cells within 30 days in the presence of exogenous or endogenous Activin A.

Despite the high efficiency in retinal induction from human ES cells in our neuroepithelial cyst model, what factors are responsible for generating majority of optic vesicle stage cells in our model remains unclear. In our lab Andrea Meinhardt showed that mouse ES cell-derived neuroepithelial cysts were probably a mixture of

midbrain and hindbrain progenitor cells, no eyefield cells. Thus a thought that the specific eyefield induction from human ES cells is related to their later developmental stage which is distinct from that of mouse ES cells came to mind. So I checked the regional identity of neuroepithelial cysts derived from mouse EpiS cells which reflect a similar late epiblast origin as human ES cells do. However, mouse EpiS cell-derived neuroepithelial cysts showed mainly RX^-, $OTX2^-$, partially $PAX6^+$ and partially $EN1^+$ at Day 3 by immunostaining. It's unlikely that mouse EpiS cell-derived neuroepithelial cysts enter eyefield and they might be heterogeneous in cell composition. Next, I did some preliminary experiments to check whether certain growth factors are involved in the determination of retinal identity in human ES cell system. For example, in previous 2D induction protocols, IGF-1 (10 ng/ml) contributed to directing human ES cells to a retinal progenitor identity(Lamba et al., 2006). To test the possible role of IGF-1, I added the pharmacological inhibitor, AG 1024, to the N2B27 medium at Day 0. In the presence of AG1024, the fraction of $PAX6^+$ cysts at Day 5 was reduced from 99% to 33.9±1.9%. The $PAX6^-$ cysts failed to achieve a pseudostratified architecture, and rather formed single cell layered epithelial cysts (Figure 3.19). In addition, the expression of RX and OTX2 was also extremely low or absent in these $PAX6^-$ cysts. ZO-1 expression was still mainly seen at the apical-lateral border of the cysts indicating that cell polarity was preserved (Figure 3.19 b). However, AG1024 could not only inhibit IGF-1 receptor kinase signaling but also insulin receptor kinase signaling. Therefore the preliminary experiments only suggest that IGF-1/insulin signaling might be required for the formation of a pseudostratified, optic vesicle stage neuroepithelium in our neuroepithelial cyst model. Further studies are clearly required to elucidate other critical components underlying the effect of Matrigel induced differentiation.

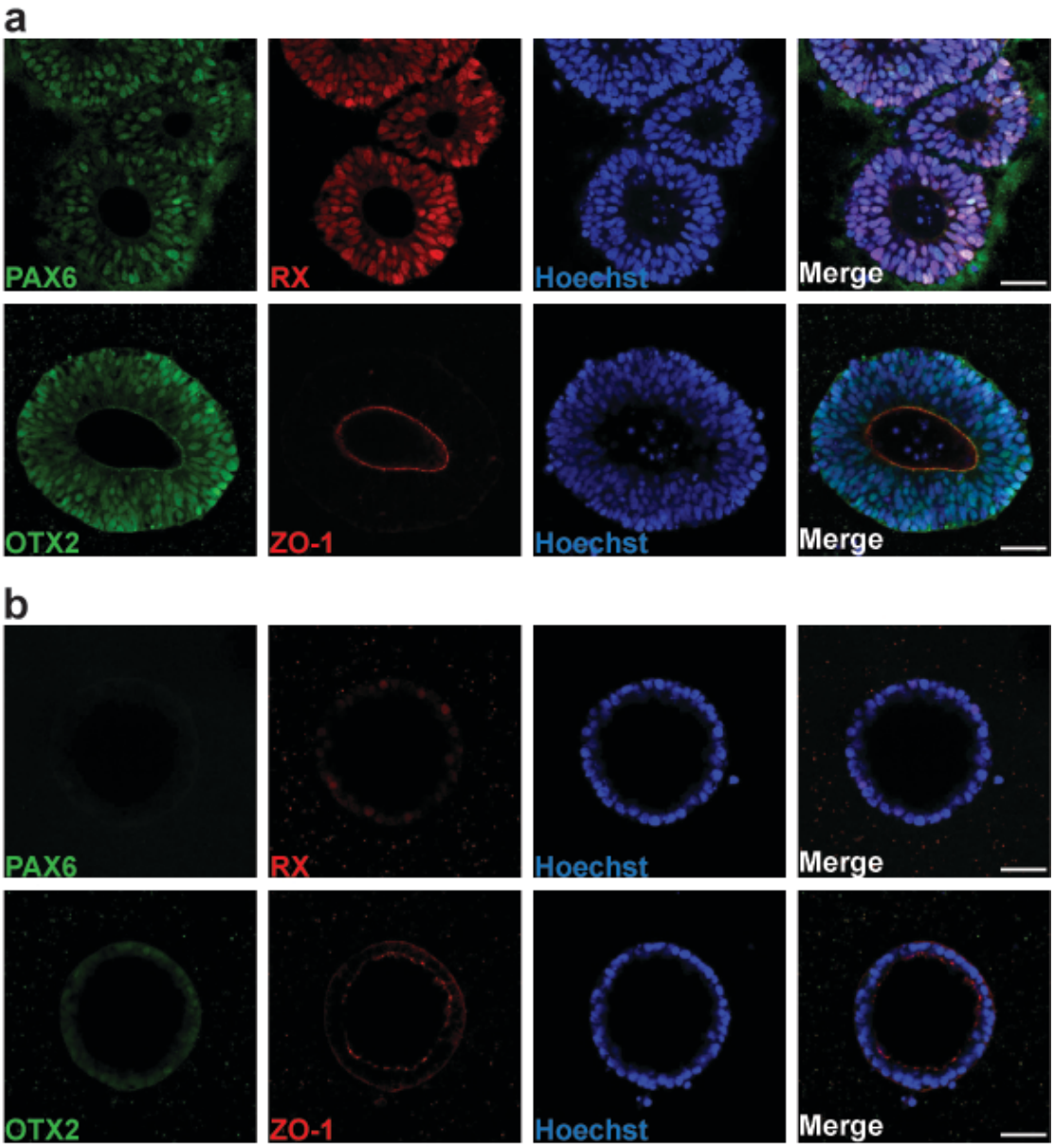

Figure 3.19 Possible involvement of IGF-1 signaling in optic vesicle stage neuroepithelium formation during human ES cell differentiation in Matrigel.

Human ES cell-derived neuroepithelial cysts at Day 5 were co-stained with PAX6 and RX antibodies (upper row) or OTX2 and ZO-1 antibodies (lower row). (a) Cysts generated in the presence of DMSO as a control, (b) in the presence of a pharmacological inhibitor, AG 1024 (10 μM) dissolved in DMSO. $Pax6^-$ cysts showed little RX-positive signal, indicating cells lost optic vesicle phenotype. Nuclei were counterstained with Hoechst. Scale bar, 50 μm.

It is clear that the optic vesicle stage cells formed in Matrigel that I describe here could be differentiated to cells self-organizing into rosettes with a high portion of CRX-positive photoreceptor precursor cells in a 60-day timescale, indicating that human ES cell-derived optic vesicle stage cells in the Matrigel are open to forming neural retina. However, the human eyefield cysts are not restricted to forming neural retina, but also forming RPE highly efficiently. I then focus more on the RPE determination, which is one of the earliest differentiated cell types during retinal development. In terms of RPE induction, it is clearly important that I start the induction with a uniform population of optic vesicle stage cells, which derives from high quality human ES cell propagation combined with neuroepithelial cyst formation in Matrigel. The subsequent transwell filter culture in RPE differentiation-promoting medium then favors the formation of a polarized RPE cell sheet as a monolayer. We believe the combination of Matrigel-based 3D followed by transwell filter-based 2D culturing accurately recapitulates the *in vivo* developmental process of neuroepithelium at optic vesicle stage toward RPE monolayer(Martinez-Morales et al., 2004a). Furthermore, the studies confirm that TGF-β family members such as Activin can substitute for the extraocular mesenchyme to promote RPE specification as predicted from studies in chick embryos and from previous embryoid body-based differentiation protocols(Fuhrmann et al., 2000; Idelson et al., 2009; Meyer et al., 2011). Taken together, my results show that recapitulating the *in vivo* developmental milieu, not only via soluble growth factors, but also by mimicking the extracellular matrix conditions that promote epithelium formation is crucial for setting up efficient *in vitro* models for human ES cell differentiation.

In conclusion, the uniformity and patternability of the neuroepithelia was evidenced in the human ES cell system where cysts achieve eyefield identity and where we could subsequently quantitatively generate neural retina epithelium or retinal pigment epithelium dependent on the culture media. These experiments open the path for future challenging experiments reconstituting neuroepithelial patterning directly in neuroepithelial cysts using defined soluble factors. Such experiments were previously inaccessible, since complex neuroepithelial aggregate cultures underwent their own self-organization(Eiraku et al., 2011; Eiraku et al., 2008). This model can also support the directed generation of a high percentage of retinal cells, especially RPE cells which have morphological and functional properties highly characteristic of native

RPE cells, from human pluripotent stem cells through a neuroepithelial cyst stage. This work has clear implications for the use of human pluripotent stem cells for studying normal and diseased human RPE, and for advancing therapeutic strategies to treat blindness.

Chapter 4

Materials and methods

4.1 List of reagents and media preparation

The regular chemicals were purchased from Sigma, Invitrogen, Merck or Roth.

Reagents	**Supplier**	**Cat. No.**	**Comments**
mTeSR1	StemCell Technologies	05870	
mFreSR	StemCell Technologies	05854	
Dispase	StemCell Technologies	07923	Aliquots stored at -20°C
BD Matrigel hESC-qualified matrix	BD Biosciences	354277	Aliquots stored at -20°C/-80°C
Matrigel	BD Biosciences	354234	Aliquots stored at -20°C/-80°C
Growth factor-reduced-Matrigel	BD Biosciences	356230	Aliquots stored at -20°C/-80°C
Cell recovery solution	BD Biosciences	354253	
TrypLE	Invitrogen	12563	
DMEM/F-12	Gibco	31330-038	
DMEM/F12+GlutaMax-I	Gibco	31331-028	
DMEM+GlutaMax-I	Gibco	31966-021	
Knockout serum replacement	Gibco	10828-028	Aliquots stored at -20°C
Non-essential amino acid	Gibco	11140	
Neurobasal medium	Gibco	21103-049	
B27-supplement	Invitrogen	17504-044	Aliquots stored

			at -20°C
Transferrin	Sigma-Aldrich	T1428	
Sodium pyruvate MEM	Gibco	11360-039	
L-Glutamine 200 mM	Invitrogen	25030-024	Aliquots stored at -20°C
Penicillin-Streptomycin	Invitrogen	15140-122	Aliquots stored at -20°C
Recombinant Human/Mouse/Rat Activin	R&D	338-AC-010	Dissolved in PBS/0.1% BSA. Aliquoted stock concentration: 10 µg/ml. Flash frozen in liquid nitrogen and stored at -80°C.

Table 4.1 List of reagents used.

Cat. No.: Catalog number.

N2-supplement:
3.468 ml DMEM/F12+GlutaMax^{TM}-I (Gibco 31331-028)
500 µl Transferrin (100 mg/ml, aliquots stored at -20°C)
335 µl BSA (75 mg/ml dissolved in PBS, aliquots stored at -20°C)
16.5 µl Progesterone (0.6 mg/ml dissolved in ethanol, aliquots stored at -20°C)
50 µl Putrescine (160 mg/ml, aliquots stored at -20°C)
5 µl Selenium (3 mM, aliquots stored at -20°C)
625 µl Insulin (20 mg/ml, aliquots stored at -20°C)
(The complete N2-supplement should be aliquoted and stored at -20°C for up to 3 weeks.)

N2B27 medium:
50 ml DMEM/F12+GlutaMaxTM-I (Gibco 31331-028)
50 ml Neurobasal medium (Gibco 21103-049)
1 ml B27-supplement
0.5 ml N2-supplement
100 µl b-mercaptoethanol solution (10 µl b-mercaptoethanol in 1.4 ml H2O)
250 µl Pyruvate+Glutamine solution (8.25 ml Pyruvate mixed with 5.5 ml Glutamine, aliquots stored at -20°C)
1 ml Penicillin-Streptomycin
(The complete N2B27 medium should be kept at 4°C for up to 1 week.)

RPE medium:
200 ml DMEM+GlutaMax^{TM}-I (Gibco, 31966-021)
50 ml Knockout^{TM} Serum Replacement (Gibco, 10828-028)
2.5 ml Non-Essential Amino Acid (Gibco, 11140)
1.25 ml Glutamine+b-mercaptoethanol (5 ml 200mM Glutamine+7 µl b-mercaptoethanol)
(The complete RPE medium should be aliquoted and stored at -20°C. Thawed RPE medium could be stored at 4°C for up to 2 weeks.)

4.2 Cell culture

4.2.1 Mouse EpiS cell culture

Mouse EpiS cell line E14 (gift of Ian Chambers, University of Edinburgh, Edinburgh, UK) was cultured in N2B27 medium supplemented with Activin A (R&D, 20 ng/ml) and FGF2 (10 ng/ml) on Fibronectin coated plates. N2B27 medium consisted of DMEM/F12+GlutaMax^{TM} (Gibco), neurobasal medium (Gibco), 0.5×B27 supplement (Gibco), 0.5×N2 supplement, 0.1 mM β-mercaptoethanol and 0.2 mM L-Glutamine, prepared as described(Pollard et al., 2006). The cells were passaged using Accutase (Sigma).

4.2.2 Human ES and iPS cell culture

Human ES cell lines H9, H1 (WISC Bank)(Thomson et al., 1998) and one iPS cell line O27-08 (gift of Yasuhiro Takashima and Austin Smith, University of Cambridge, Cambridge, UK) were cultured in mTeSR1 medium (StemCell Technologies) on BD Matrigel hESC-qualified Matrix (BD Biosciences)-coated plates.(Ludwig et al., 2006a) The human ES cells and human iPS cells expressed OCT4 and SSEA4, confirming the undifferentiated state. Cells were passaged every 5-6 days using Dispase (StemCell Technologies), and morphologically distinguishable differentiated cells were mechanically removed at each passage. For storage, the human ES cell colonies were suspended in mFreSR^{TM} (StemCell Technologies), frozen in an isopropanol freezing container at -80°C overnight and transferred into liquid nitrogen the next day. To improve cell survival during thawing, the Rho kinase inhibitor, Y-27632 (Calbiochem), was added in the culture medium during the first 24 hours after plating.

4.2.3 Detailed protocol for human ES and iPS cell passaging

Human ES and iPS cells grown in mTeSR1 are ready to passage when the colonies are large, beginning to merge, and have centers that are dense and phase-bright compared to their edges. There is an approximate 24-hour window that is optimal for passaging. If colonies are passaged too early or too frequently, the cells may not attach well, yields will be decreased and cells may start to differentiate. If colonies are passaged too late, the culture will begin to show signs of differentiation (characterized by the emergence of cell types with different morphologies). Less than 5% spontaneous differentiation in culture is considered as high quality. The detailed protocol for passaging is shown below:

1. Warm aliquoted mTeSR1 (StemCell Technologies 05870), Dispase (StemCell Technologies 07923), and DMEM/F-12 (Gibco 31330-038) to room temperature (15 - 25°C). Coat a six-well plate with BD Matrigel hESC-qualified matrix (BD Biosciences 354277) diluted in DMEM/F12 as required in the datasheet of different batches of hESC-qualified Matrigel (1 ml per well for coating). The coated plate is kept at room temperature for at least 1 hour before using.

2. Use a microscope to visually identify regions of differentiation. Morphologically distinguishable differentiated cells are mechanically removed using a scalpel while viewing under a microscope at 5x magnification.

3. After cutting away differentiated cells, aspirate medium from the human ES or iPS cell culture and rinse with DMEM/F12 (2 ml/well).

4. Add 1 ml per well of Dispase. Place at 37°C for 7 minutes. After incubation the colony edges will appear slightly folded back but the colonies should remain attached to the plate.

5. Remove Dispase, and gently rinse each well 2 - 3 times with 2 ml of DMEM/F-12 per well to dilute away any remaining dispase.

6. Add 1 ml/well of mTeSR1 and scrape colonies off with a cell scraper (Corning Costar 3010). Ensure that cells are maintained as aggregates.

7. Remove the Matrigel in the coated six-well plate. Plate the human ES or iPS cell aggregates with mTeSR1 onto the new plate (2 ml/well). If the colonies are at an optimal density, the cells can be split every 4 - 7 days using 1:6 to 1:10 splits (i.e. the aggregates from 1 well of a 6-well plate can be plated in 6 - 10 wells of a 6-well plate). If the colonies are too dense or too sparse, adjust the split ratio accordingly.

8. Move the plate in several quick, short, back-and-forth and side-to-side motions to disperse cells across the surface of the wells to ensure that newly seeded colonies are evenly dispersed across the entire surface of a Matrigel-coated plate rather than clumped in the middle. Place the plate in a 37°C incubator.

4.3 Cell differentiation experiments

4.3.1 Differentiation of pluripotent stem cells in the neuroepithelial cyst model

Mouse EpiS cell clumps or human pluripotent stem cell clumps were embedded in Matrigel. 30-50 μl of Matrigel containing the cells was added per square centimeter of growth surface. After gelling at 37°C for 10 min, cells embedded in the Matrigel layer

were cultured in neural induction medium N2B27. In separate experiments, Collagen I (BD Biosciences, 1.8 mg/ml) or Laminin/Entactin (BD Biosciences, 10 mg/ml) gel was used instead of Matrigel. If required, human ES cell clumps were pre-treated with βI-integrin blocking antibody AIIB2 (DSHB) or IgG control antibody (100 μg/ml) for 1 hour in a 37°C, 5% CO_2 incubator before embedding in Matrigel. AIIB2 or control antibodies were then kept in N2B27 medium at a concentration of 10 μg/ml during differentiation in neuroepithelial cyst model.

4.3.2 Detailed protocol for differentiation of human ES and iPS cells in the neuroepithelial cyst model

When human ES and iPS cells grown in mTeSR1 are ready to passage, it's also the timing to start differentiation experiments.

1. Warm aliquoted Dispase, DMEM/F-12 and N2B27 medium to room temperature (15 - 25°C). Thaw aliquoted Matrigel (BD Biosciences 354234) on ice. N2B27 medium is consisted of DMEM/F12+GlutaMax™-I (Gibco 31331-028), neurobasal medium (Gibco 21103-049), 0.5×B27 supplement, 0.5×N2 supplement, 0.1 mM β-mercaptoethanol and 0.2 mM L-Glutamine, prepared as described in Chapter 4.1.

Repeat step 2-5 in the protocol for passaging the cells (Page 1). It's critical to remove differentiated cells before Dispase treatment to make sure cyst preparation starts from pure pluripotent stem cells.

6. Add 1 ml/well of N2B27 medium and scrape colonies off with a cell scraper (Corning Costar 3010). Ensure that cells are maintained as aggregates.

7. Transfer the detached cell aggregates (diameter: 50-100 μm) from one well of a six-well plate (~1×10^6 cells) to a 15 ml falcon tube.

8. Centrifuge the 15 ml tube containing the aggregates at 700 x *g* for 1 minutes at room temperature (15 - 25°C).

9. Aspirate the supernatant. For each well of human ES or iPS cell aggregates collected in the 15 ml tube, add 10-15 μl N2B27 medium. Place the 15 ml tube onto ice.

10. Add 100-150 μl Matrigel into the 15 ml tube on ice. Resuspend pellet by gently pipetting up and down with a P200 micropipette (~3 times). Cut the pipette tip using the scissors to avoid destroying the cell clumps during resuspending in Matrigel. Cyst formation is high-density dependent. The volume of Matrigel to be used is adjustable.

11. Around 50 μl of Matrigel containing the cell clumps is added onto one glass bottom dish (MatTek Corporation P35G-1.5-14-C). Ensure the Matrigel covers the majority of the glass part of the dish to make a thin layer of Matrigel with cell clumps in. Avoid a thick Matrigel drop. Place the glass bottom dishes at 37°C for gelling (6-8 minutes).

12. Add 2 ml of N2B27 medium in each glass bottom dish. The medium is changed every 3-5 days.

4.3.3 Differentiation of neural retina or RPE cells from human pluripotent stem cell-derived neuroepithelial cysts on transwell filters

Human ES cell- or human iPS cell-derived neuroepithelial cysts at Day 5 were taken out of the Matrigel using Cell Recovery Solution (BD Biosciences). To get rid of the few non-cyst cells, large cysts were permitted to sink down to the bottom of the tube by gravity. Then the cysts were treated with TrypLE™ (Invitrogen), followed by gentle trituration to achieve single cell suspension. 40 μm-cell strainer (BD Biosciences) was used to exclude big clumps after TrypLE™ treatment. Dispersed cells were resuspended in N2B27 medium and plated onto growth factor-reduced-Matrigel (BD Biosciences)-coated 6.5 mm Transwell® with 0.4 μm Pore Polyester Membrane Insert (Corning Costar) at a density of $2\text{-}4\times10^5$ cells/well. For neural retina differentiation, the cells were kept in N2B27 medium. The medium was changed every 2-3 days. For RPE differentiation, at Day 6, attached cells on transwell filters were washed twice with RPE medium---DMEM+GlutaMax™ medium supplemented with 20% Knockout™ serum replacement (Gibco), non-essential amino acids, 1 mM L-Glutamine and 0.1 mM β-mercaptoethanol. The cells were then kept in RPE medium with or without 100 ng/ml human Activin A. In the experiments of inhibiting TGF-β signaling, SB 431542 (Sigma, 8 μM) was added in cultures from Day 6 to 25. The medium was changed every 2-3 days.

4.3.4 Detailed protocol for differentiation of RPE cells on transwell filters

Human ES or iPS cell-derived cysts at Day 5 (The day when cell clumps were embedded in Matrigel was counted as Day 0.) were used for further differentiation on transwell inserts.

1. Warm aliquoted TrypLE™ (Invitrogen 12563), PBS and N2B27 medium to room temperature (15 - 25°C).

2. Coat the 6.5 mm Transwell® insert (Corning Costar 3470, 0.4 µm Pore Polyester Membrane Insert) with growth factor-reduced-Matrigel (BD Biosciences 356230). Growth factor-reduced-Matrigel is diluted in DMEM/F12 (1:40, 100 µl per insert) for coating. The coated plate is kept at room temperature for at least 1 hour before using.

3. Aspirate N2B27 medium from the cyst culture and rinse with PBS (2 ml/dish).

4. Prepare a 15 ml falcon tube on ice. Add 5 ml ice-cold Cell Recovery Solution (BD Biosciences 354253) in the tube.

5. Aspirate PBS in one dish and take off the glass coverslip on the bottom of the dish using scalpel. Scrape off the Matrigel drop from the coverslip and put the Matrigel containing cysts into the 15 ml falcon tube with ice-cold Cell Recovery Solution in. Taking the glass coverslip off the dish is just to make the Matrigel drop easily accessible. Collect Matrigel drops from 4-5 dishes into one falcon tube.

6. Place the falcon tube on ice for 30-45 minutes. Tip the tube up and down from time to time.

7. When there are no visible Matrigel pieces in Cell Recovery Solution and all the cysts are released, keep the tube standing in ice for 10-15 minutes. Large cysts are permitted to sink down to the bottom of the tube by gravity to get rid of the few non-cyst cells. Cysts still remain as intact cysts at this step.

8. Aspirate Cell Recovery Solution from the tube without destroying the soft cyst pellet and add 2 ml PBS.

9. Centrifuge the 15 ml tube containing the cysts at 300 x *g* for 1 minute at room temperature (15 - 25°C).

10. Aspirate the supernatant. Add 1 ml TrypLE. pipet it up and down with a P1000 micropipette 1-2 times to resuspend the cysts. Place the 15 ml tube into 37°C water bath for 4 minutes. Very gently flip the tube during the 4-min incubation. Please avoid cysts sticking to the wall of the tube.

11. After the 4-min incubation in water bath, pipet the remaining cysts up and down with a P1000 micropipette several times to better dissociate the cysts until there are no visible cell clumps. Please keep the pipetting step shorter than 1 minute.

12. Centrifuge the 15 ml tube containing the cysts at 1000 x *g* for 2 minutes at room temperature (15 - 25°C).

13. Aspirate the supernatant. Add 4 ml N2B27 medium. Resuspend the cells by pipetting.

14. Rinse a 40 μm-cell strainer (BD Biosciences) with 1 ml N2B27 medium. Let the resuspended cells go through the cell strainer to get rid of the big clumps that are not well dissociated. Rinse the cell strainer again with 1 ml N2B27 medium. Transfer the cells that passed through the sieve (~6 ml) from the collecting 50 ml falcon tube to a 15 ml falcon tube.

15. Count the cells using a hemocytometer.

16. Centrifuge the 15 ml tube containing the dispersed cells at 1000 x *g* for 3 minutes at room temperature (15 - 25°C).

17. Aspirate the supernatant. Resuspend the cells in N2B27 medium so that you will be able to plate 2-4×10^5 cells in 100 μl. Aspirate the growth factor-reduced-Matrigel in the Transwell insert and plate 100 μl of the cells onto it at a density of 2-4×10^5 cells/well. The lower chamber of the transwell is filled with 600 μl of N2B27 medium. The efficiency of RPE differentiation is density dependent. The best seeding density might differ between different hands based on the cell viability after TrypLE treatment. A titration experiment for optimizing the seeding density (range from 1 to 10×10^5 cells/well) is necessary.

18. One day after cell seeding (counted as Day 6), attached cells are rinsed twice with RPE medium (see below). The cells are then kept in RPE medium with or without

100 ng/ml human Activin A (R&D 338-AC-010). The medium is changed every 2-3 days. The emergence of pigmented cells starts from Day 15- Day 25 (It varies on different cell lines).

4.4 Immunocytochemistry

Cells or cysts were fixed with freshly made 4% paraformaldehyde (PFA) for 20 min at room temperature (RT), followed by antigen retrieval (if necessary, Citrate buffer, 70°C, 30 min), quenching (1×PBS, 100mM Glycine, 0.3% Triton X-100) and blocking (1×PBS, 0.5% BSA, 0.3% Triton X-100). Immunostaining was performed in blocking buffer and each antibody reaction was done overnight at 4°C.

For EdU incorporation, human ES cell-derived cysts at Day 5 were incubated with EdU for 1 hour, while RPE preparations on transwell filters were incubated with EdU for 24 hours. Click-iT™ EdU Alexa Fluor® 647 Imaging Kit (Invitrogen) was used for detection.

Cell nuclei were counterstained with Hoechst 33342 (1-5 μg/ml, Sigma). F-actin in cells was stained with Alexa Fluor 647 Phalloidin (1:200, Invitrogen).

4.4.1 Primary antibodies

Antigen	**Description**	**Dilution**	**Supplier/Reference**
SOX1	Goat polyclonal	1:500	R&D
CD133	Rat polyclonal	1:100	Gift of Wieland Huttner, MPI-CBG
CD133	Mouse monoclonal	1:50	Miltenyi Biotec
NESTIN	Rabbit polyclonal	1:500	Abcam
SOX2	Rabbit polyclonal	1:100	Zymed
ZO-1	Rabbit polyclonal	1:100	BD Biosciences

PAX6	Rabbit polyclonal	1:200	HISS Diagnostics
PAX6	Mouse monoclonal	1:20	McHedlishvili et al., 2007(McHedlishvili et al., 2007)
OTX2	Rabbit polyclonal	1:200	Abcam
CHX10	Sheep polyclonal	1:200	Chemicon
MITF	Mouse monoclonal [C5]	1:50	Abcam
RPE65	Mouse monoclonal	1:500	Millipore
BESTROPHIN	Mouse monoclonal	1:1000	Millipore
Human nuclei	Mouse monoclonal	1:50	Millipore
EEA1	Mouse monoclonal	1:1000	Gift of Marino Zerial, MPI-CBG
GFP	Goat polyclonal	1:400	Rockland
OCT4	Rabbit polyclonal	1:100	Abcam
SSEA1	Mouse monoclonal, IgM	1:50	DSHB
SSEA4	Mouse monoclonal	1:50	DSHB

Table 4.2 List of commercial primary antibodies used.

Antibodies against RX and CRX were raised in rabbits immunized with a portion of human RX (residues 216-258) or human CRX (residues 112-259) tagged with GST and affinity-purified against the corresponding MBP-RX or MBP-CRX fusion proteins respectively. The immunoreactivity of each antibody was confirmed by immunostainings on mouse tissues of corresponding stage as a positive control (Figure 3.2 and 3.6). Detailed information is shown below:

1. RX antibody

a. Antigen info

DNA sequence accession: BC156201

Amino acid sequence (with the region that was used as antigen marked underlined):

MHLPGCAPAMADGSFSLAGHLLRSPGGSTSRLHSIEAILGFTKDDGILGTFPAE
RGARGAKERDRRLGARPACPKAPEEGSEPSPPPAPAPAPEYEAPRPYCPKEPG
EARPSPGLPVGPATGEAKLSEEEQPKKKHRRNRTTFTTYQLHELERAFEKSHY
PDVYSREELAGKVNLPEVRVQVWFQNRRAKWRRQEKLEVSSMKLQDSPLLS
FSRSPPSATLSPLGAGPGSGGGPAGGALPLESWLGPPLPGGGATALQSLPGFG
PPAQSLPASYTPPPPPPPFLNSPPLGPGLQPLAPPPPSYPCGPGFGDKFPLDEAD
PRNSSIAALRLKAKEHIQAIGKPWQAL

b. Antibody info (Project M3525)

Concentration: 0.39 mg/ml

Dilution for immunofluorescence: 1:1000

c. Vendor

Charles river

2. CRX antibody

a. Antigen info

DNA sequence accession: BX117143

Amino acid sequence (with the region that was used as antigen marked underlined):

MMAYMNPGPHYSVNALALSGPSVDLMHQAVPYPSAPRKQRRERTTFTRSQL
EELEALFAKTQYPDVYAREEVALKINLPESRVQVWFKNRRAKCRQQRQQQK
QQQQPPGGQAKARPAKRKAGTSPRPSTDVCPDPLGISDSYSPPLPGPSGSPTTA
VATVSIWSPASESPLPEAQRAGLVASGPSLTSAPYAMTYAPASAFCSSPSAYG
SPSSYFSGLDPYLSPMVPQLGGPALSPLSGPSVGPSLAQSPTSLSGQSYGAYSP
VDSLEFKDPTGTWKFTYNPMDPLDYKDQSAWKFQIL*

b. Antibody info (Project M3480)

Concentration: 0.5 mg/ml

Dilution for immunofluorescence: 1:5000

c. Vendor

MPI-CBG antibody facility

4.4.2 Secondary antibodies

Description	**Conjugate**	**Dilution**	**Supplier**
Donkey anti-mouse, IgG	Alexa Fluor 555	1:200	Invitrogen
Donkey anti-mouse, IgG	Alexa Fluor 647	1:200	Invitrogen
Donkey anti-rabbit, IgG	Alexa Fluor 488	1:200	Invitrogen
Donkey anti-rabbit, IgG	Alexa Fluor 647	1:200	Invitrogen
Donkey anti-sheep, IgG	Alexa Fluor 555	1:200	Invitrogen
Donkey anti-rat, IgG	Alexa Fluor 488	1:200	Invitrogen
Donkey anti-goat, IgG	Alexa Fluor 488	1:200	Invitrogen
Donkey anti-goat, IgG	Alexa Fluor 555	1:200	Invitrogen
Goat anti-mouse, IgM	Alexa Fluor 555	1:200	Invitrogen

Table 4.3 List of secondary antibodies used.

4.4.3 Microscopy

Cells were imaged using a Zeiss LSM 510 confocal microscope, Leica TCS SPE confocal microscope or Zeiss Axiovert 200 microscope. Fiji and Adobe Illustrator were used for data analysis and image processing.

4.5 RT-PCR analyses

Total RNA was extracted from undifferentiated or differentiating human ES cells using RNeasy (Qiagen), treated with RNase-free DNase I (Invitrogen) and reverse-transcribed with SuperScript II (Invitrogen). The synthesized cDNA was amplified with gene-specific primers (shown in the table below). PCR was carried out with Taq DNA Polymerase with denaturation 94°C-20 s, annealing 55°C-30 s, extension 72°C-60 s for 35 cycles.

Gene	**Primers used for RT-PCR (F: Forward / R: Reverse)**	
OCT4	F	5'-AGTGAGAGGCAACCTGGAGA-3'
	R	5'-GTGAAGTGAGGGCTCCCATA-3'
SOX1	F	5'-CAATGCGGGGAGGAGAAGTC-3'
	R	5'-CTCTGGACCAAACTGTGGCG-3'
PAX6	F	5'-AACAGACACAGCCCTCACAAACA-3'
	R	5'-CGGGAACTTGAACTGGAACTGAC-3'
RX	F	5'-GAATCTCGAAATCTCAGCCC-3'
	R	5'-CTTCACTAATTTGCTCAGGAC-3'
SIX3	F	5'-ACCACAAGTTCACCAAGGAGTCTC-3'
	R	5'-ATTCCGAGTCGCTGGAGGTTAC-3'
MITF	F	5'-GACAGAAGAAACTGGAGCACGC-3'

	R	5’-TCCGAGGTTGTTGTTGAAGGTG-3’
CHX10	F	5’-GCTCGGATTCTGAAGATGTTTCC-3’
	R	5’-TGCCTCCAGCGACTTTTTGTG-3’
CRX	F	5’-ATGATGGCGTATATGAACCC-3’
	R	5’-TCTTGAACCAAACCTGAACC-3’
BF-1	F	5’-ACTCAAAACTCGCTGGGCAAC-3’
	R	5’-CGTGGGGGAAAAAGTAACTGG-3’
PAX2	F	5′-ATGTTCGCCTGGGAGATTCG-3′
	R	5′-GCAAGTGCTTCCGCAAACTG-3′
HOXB1	F	5′-TCAGAAGGAGACGGAGGCTA-3′
	R	5′-GTGGGGGTGTTAGGTTCTGA-3′
HOXC5	F	5′-TCGGGGTGCTTCCTTGTAGC-3′
	R	5′-TTCGTGGCAGGGACTATGGG-3′
GAPDH	F	5’-GGGGAGCCAAAAGGGTCATCATCT-3’
	R	5’-GAGGGGCCATCCACAGTCTTCT-3’

Table 4.4 List of primers used for RT-PCR.

4.6 Electron microscopic analyses

Cells were fixed and processed on the transwell filters. They were fixed with 2% glutaraldehyde and 2% PFA in 50 mM HEPES overnight at 4°C. After several washes in 100 mM HEPES and PBS they were postfixed with 1% OsO_4/PBS for 2 hours on ice, washed with PBS and water, and *en bloc* contrasted with 1% uranyl acetate in water, again for 2 hours on ice. Samples were dehydrated in a graded ethanol series, infiltrated in ethanol/epon mixtures (1:3, 1:1, 3:1) and in pure epon (2x) and cured at 60°C for 24 hours. Samples were cut to small pieces (1-2 mm), remounted for cross-sectioning of the RPE layer on empty epon dummy blocks and cured for another 24 hours at 60°C. Ultrathin sections were stained with lead citrate and uranyl acetate and inspected at a FEI Morgagni 268 D transmission electron microscope at 80 kV.

4.7 Measurement of transepithelial resistance

The transepithelial resistance of the human ES cell-derived RPE cells growing on transwell filters and the empty transwell filters only coated with growth factor-reduced-Matrigel as a control was measured by using an EVOM epithelial voltohmmeter (World Precision Instruments, Hamden, CT) with a pair of chopstick electrodes.

4.8 Phagocytosis analyses using retinal explant co-culture model

The transwell filter (diameter: 6.5 mm), on which human ES cell-derived RPE was grown, was excised and transferred to a bigger transwell filter (diameter: 24 mm) with the cells facing up for easier handling. Neural retinal explants from transgenic mice expressing human RHODOPSIN-GFP(Chan et al., 2004) were dissected out in PBS and oriented on top of the RPE cell sheet to make the outer segments localize adjacent to the apical surface of human ES cell-derived RPE. By adding one small drop of low-melting-point agarose gently on top of the retinal explant, the outer segment layer better contacted the RPE. 1 ml of N2B27 medium supplemented with 10% FBS was added to the lower chamber of the transwell so that the medium just touched the

surface of the transwell filters. The human ES cell-derived RPE plus mouse retina composites were fixed in 4% PFA for 1 hour at RT after 24 hours of co-culture, followed by immersion in 30% sucrose at 4°C overnight and subsequent embedding in Tissue-Tek O.C.T.^{TM} Compound (Sakura). The thickness of cross-sections was 10 μm.

4.9 In situ hybridization on cyst cryosections

Human ES cell-derived cysts at representative time points were fixed in 4% fresh PFA for 20 min at RT, washed in PBS, equilibrated in 30% sucrose and frozen in Tissue-Tek O.C.T.^{TM} Compound. *In situ* hybridization on cryosections of 10 μm thickness was performed as described(Schnapp et al., 2005). Briefly, the sections were washed in PBS/0.1% Tween, hybridized with 500 ng/ml DIG-labeled probe in hybridization buffer (50% formamide, 10% dextran, 5x SSC, 0.1% Tween, 1 mg/ml yeast RNA, 100 μg/ml heparin, 1x Denhardt's, 0.1% CHAPS, 5 mM EDTA) overnight at 70°C. Slides were washed three times an hour and then overnight at 70°C in 5x SSC buffer (50% formamide, 5x SSC, 0.1% Tween), followed by twice an-hour washes at 70°C in post-hybridization buffer (50% formamide, 2x SSC, 0.1% Tween). Slides were further washed twice 5 min and once 20 min at RT in maleic acid buffer (100 mM maleic acid pH 7.5, 150 mM NaCl, 0.1% Tween), blocked in maleic acid buffer plus 1% blocking reagent (Roche) for an hour at RT, and then incubated overnight at 4°C with anti-DIG antibody (1:5000, Roche) in this blocking solution. Slides were washed 5x 10 min with maleic acid buffer and 2x 10 min with alkaline phosphatase buffer (100 mM Tris pH 9.5, 50 mM $MgCl_2$, 100 mM NaCl, 0.1% Tween). Each Slide was overlaid with BM purple (Roche) for 6-48 hours at 37°C. The reaction was stopped in cold PBS/1 mM EDTA and the slides were mounted in 50% glycerol.

Sense and antisense probes of *OCT4* and *RX* for *in situ* hybridizations were obtained by RT-PCR from total RNA of undifferentiated or differentiated human ES cells. Primers used to amplify the fragments of *OCT4* (database accession no. NM_203289) and *RX* (database accession no. NM_013435) cDNA were shown in the table below.

Sense and antisense probes of *PAX6* were prepared from the Full Length cDNA Clone IRATp970B0617D (imaGenes, database accession no. BC011953).

Images of sectioned samples were acquired with inverted microscope Axiovert 200. Mosaix images were stitched using the Axiovision software without any manipulation of images.

Gene	**Primers used for *in situ* hybridization probes (F: Forward / R: Reverse)**	
OCT4	F	5'-AAGGATGTGGTCCGAGTGTGGTTC-3'
	R	5'-TAGAAGGGCAGGCACCTCAGTTTG-3'
RX	F	5'-AATCGTCCCCATTCCGAACG-3'
	R	5'-TGGTCATCCTTTTCCCAAGTCG-3'

Table 4.5 List of primers used for *in situ* hybridization probes.

4.10 Statistical analyses

Values are expressed as means±s.e.m.. All sets of experiments were performed at least in three replicates. For quantification, 100-200 cysts or 500-1000 cells were scored per marker within random fields at each experiment. Statistical analyses were performed with IGOR PRO 6.1.

References

Bao, S., Tang, F., Li, X., Hayashi, K., Gillich, A., Lao, K., and Surani, M.A. (2009). Epigenetic reversion of post-implantation epiblast to pluripotent embryonic stem cells. Nature *461*, 1292-1295.

Baumer, N., Marquardt, T., Stoykova, A., Spieler, D., Treichel, D., Ashery-Padan, R., and Gruss, P. (2003). Retinal pigmented epithelium determination requires the redundant activities of Pax2 and Pax6. Development *130*, 2903-2915.

Brons, I.G., Smithers, L.E., Trotter, M.W., Rugg-Gunn, P., Sun, B., Chuva de Sousa Lopes, S.M., Howlett, S.K., Clarkson, A., Ahrlund-Richter, L., Pedersen, R.A.*, et al.* (2007). Derivation of pluripotent epiblast stem cells from mammalian embryos. Nature *448*, 191-195.

Buchholz, D.E., Hikita, S.T., Rowland, T.J., Friedrich, A.M., Hinman, C.R., Johnson, L.V., and Clegg, D.O. (2009). Derivation of functional retinal pigmented epithelium from induced pluripotent stem cells. Stem Cells *27*, 2427-2434.

Carpenter, M.K., Inokuma, M.S., Denham, J., Mujtaba, T., Chiu, C.P., and Rao, M.S. (2001). Enrichment of neurons and neural precursors from human embryonic stem cells. Experimental neurology *172*, 383-397.

Carr, A.J., Vugler, A., Lawrence, J., Chen, L.L., Ahmado, A., Chen, F.K., Semo, M., Gias, C., da Cruz, L., Moore, H.D.*, et al.* (2009). Molecular characterization and functional analysis of phagocytosis by human embryonic stem cell-derived RPE cells using a novel human retinal assay. Mol Vis *15*, 283-295.

Chambers, S.M., Fasano, C.A., Papapetrou, E.P., Tomishima, M., Sadelain, M., and Studer, L. (2009). Highly efficient neural conversion of human ES and iPS cells by dual inhibition of SMAD signaling. Nat Biotechnol *27*, 275-280.

Chan, F., Bradley, A., Wensel, T.G., and Wilson, J.H. (2004). Knock-in human rhodopsin-GFP fusions as mouse models for human disease and targets for gene therapy. Proc Natl Acad Sci U S A *101*, 9109-9114.

Chow, R.L., and Lang, R.A. (2001). Early eye development in vertebrates. Annual review of cell and developmental biology *17*, 255-296.

Eiraku, M., Takata, N., Ishibashi, H., Kawada, M., Sakakura, E., Okuda, S., Sekiguchi, K., Adachi, T., and Sasai, Y. (2011). Self-organizing optic-cup morphogenesis in three-dimensional culture. Nature *472*, 51-56.

Eiraku, M., Watanabe, K., Matsuo-Takasaki, M., Kawada, M., Yonemura, S., Matsumura, M., Wataya, T., Nishiyama, A., Muguruma, K., and Sasai, Y. (2008). Self-organized formation of polarized cortical tissues from ESCs and its active manipulation by extrinsic signals. Cell Stem Cell *3*, 519-532.

Elkabetz, Y., Panagiotakos, G., Al Shamy, G., Socci, N.D., Tabar, V., and Studer, L. (2008). Human ES cell-derived neural rosettes reveal a functionally distinct early neural stem cell stage. Genes Dev *22*, 152-165.

Evans, M.J., and Kaufman, M.H. (1981). Establishment in culture of pluripotential cells from mouse embryos. Nature *292*, 154-156.

Finlay, B.L. (2008). The developing and evolving retina: using time to organize form. Brain research *1192*, 5-16.

Frambach, D.A., Fain, G.L., Farber, D.B., and Bok, D. (1990). Beta adrenergic receptors on cultured human retinal pigment epithelium. Invest Ophthalmol Vis Sci *31*, 1767-1772.

Fuhrmann, S. (2010). Eye morphogenesis and patterning of the optic vesicle. Current topics in developmental biology *93*, 61-84.

Fuhrmann, S., Levine, E.M., and Reh, T.A. (2000). Extraocular mesenchyme patterns the optic vesicle during early eye development in the embryonic chick. Development *127*, 4599-4609.

Furukawa, T., Morrow, E.M., and Cepko, C.L. (1997). Crx, a novel otx-like homeobox gene, shows photoreceptor-specific expression and regulates photoreceptor differentiation. Cell *91*, 531-541.

Gerrard, L., Rodgers, L., and Cui, W. (2005). Differentiation of human embryonic stem cells to neural lineages in adherent culture by blocking bone morphogenetic protein signaling. Stem cells *23*, 1234-1241.

Hatakeyama, J., and Kageyama, R. (2004). Retinal cell fate determination and bHLH factors. Seminars in cell & developmental biology *15*, 83-89.

Hatini, V., Tao, W., and Lai, E. (1994). Expression of winged helix genes, BF-1 and BF-2, define adjacent domains within the developing forebrain and retina. J Neurobiol *25*, 1293-1309.

Hu, B.Y., Weick, J.P., Yu, J., Ma, L.X., Zhang, X.Q., Thomson, J.A., and Zhang, S.C. (2010a). Neural differentiation of human induced pluripotent stem cells follows developmental principles but with variable potency. Proc Natl Acad Sci U S A *107*, 4335-4340.

Hu, Q., Friedrich, A.M., Johnson, L.V., and Clegg, D.O. (2010b). Memory in Induced Pluripotent Stem Cells: Reprogrammed Human Retinal Pigmented Epithelial Cells Show Tendency for Spontaneous Redifferentiation. Stem Cells.

Idelson, M., Alper, R., Obolensky, A., Ben-Shushan, E., Hemo, I., Yachimovich-Cohen, N., Khaner, H., Smith, Y., Wiser, O., Gropp, M.*, et al.* (2009). Directed differentiation of human embryonic stem cells into functional retinal pigment epithelium cells. Cell Stem Cell *5*, 396-408.

Inman, J.L., and Bissell, M.J. (2010). Apical polarity in three-dimensional culture systems: where to now? J Biol *9*, 2.

Kim, D.S., Lee, J.S., Leem, J.W., Huh, Y.J., Kim, J.Y., Kim, H.S., Park, I.H., Daley, G.Q., Hwang, D.Y., and Kim, D.W. (2010). Robust enhancement of neural differentiation from human ES and iPS cells regardless of their innate difference in differentiation propensity. Stem Cell Rev *6*, 270-281.

Kleinman, H.K., McGarvey, M.L., Hassell, J.R., Star, V.L., Cannon, F.B., Laurie, G.W., and Martin, G.R. (1986). Basement membrane complexes with biological activity. Biochemistry *25*, 312-318.

Kleinman, H.K., McGarvey, M.L., Liotta, L.A., Robey, P.G., Tryggvason, K., and Martin, G.R. (1982). Isolation and characterization of type IV procollagen, laminin, and heparan sulfate proteoglycan from the EHS sarcoma. Biochemistry *21*, 6188-6193.

Klimanskaya, I., Hipp, J., Rezai, K.A., West, M., Atala, A., and Lanza, R. (2004). Derivation and comparative assessment of retinal pigment epithelium from human embryonic stem cells using transcriptomics. Cloning Stem Cells *6*, 217-245.

Koch, P., Opitz, T., Steinbeck, J.A., Ladewig, J., and Brustle, O. (2009). A rosette-type, self-renewing human ES cell-derived neural stem cell with potential for *in vitro* instruction and synaptic integration. Proceedings of the National Academy of Sciences of the United States of America *106*, 3225-3230.

la Cour, M., Lin, H., Kenyon, E., and Miller, S.S. (1994). Lactate transport in freshly isolated human fetal retinal pigment epithelium. Invest Ophthalmol Vis Sci *35*, 434-442.

Lamba, D.A., Karl, M.O., Ware, C.B., and Reh, T.A. (2006). Efficient generation of retinal progenitor cells from human embryonic stem cells. Proc Natl Acad Sci U S A *103*, 12769-12774.

Ludwig, T.E., Bergendahl, V., Levenstein, M.E., Yu, J., Probasco, M.D., and Thomson, J.A. (2006a). Feeder-independent culture of human embryonic stem cells. Nat Methods *3*, 637-646.

Ludwig, T.E., Levenstein, M.E., Jones, J.M., Berggren, W.T., Mitchen, E.R., Frane, J.L., Crandall, L.J., Daigh, C.A., Conard, K.R., Piekarczyk, M.S.*, et al.* (2006b). Derivation of human embryonic stem cells in defined conditions. Nature biotechnology *24*, 185-187.

Marquardt, T., and Gruss, P. (2002). Generating neuronal diversity in the retina: one for nearly all. Trends in neurosciences *25*, 32-38.

Martin, G.R. (1981). Isolation of a pluripotent cell line from early mouse embryos cultured in medium conditioned by teratocarcinoma stem cells. Proceedings of the National Academy of Sciences of the United States of America *78*, 7634-7638.

Martin-Belmonte, F., Yu, W., Rodriguez-Fraticelli, A.E., Ewald, A.J., Werb, Z., Alonso, M.A., and Mostov, K. (2008). Cell-polarity dynamics controls the mechanism of lumen formation in epithelial morphogenesis. Current biology : CB *18*, 507-513.

Martinez-Morales, J.R., Rodrigo, I., and Bovolenta, P. (2004a). Eye development: a view from the retina pigmented epithelium. Bioessays *26*, 766-777.

Martinez-Morales, J.R., Rodrigo, I., and Bovolenta, P. (2004b). Eye development: a view from the retina pigmented epithelium. BioEssays : news and reviews in molecular, cellular and developmental biology *26*, 766-777.

McGuire, P.G., and Seeds, N.W. (1989). The interaction of plasminogen activator with a reconstituted basement membrane matrix and extracellular macromolecules produced by cultured epithelial cells. Journal of cellular biochemistry *40*, 215-227.

McHedlishvili, L., Epperlein, H.H., Telzerow, A., and Tanaka, E.M. (2007). A clonal analysis of neural progenitors during axolotl spinal cord regeneration reveals evidence for both spatially restricted and multipotent progenitors. Development *134*, 2083-2093.

Meyer, J.S., Howden, S.E., Wallace, K.A., Verhoeven, A.D., Wright, L.S., Capowski, E.E., Pinilla, I., Martin, J.M., Tian, S., Stewart, R.*, et al.* (2011). Optic vesicle-like structures derived from human pluripotent stem cells facilitate a customized approach to retinal disease treatment. Stem cells *29*, 1206-1218.

Meyer, J.S., Shearer, R.L., Capowski, E.E., Wright, L.S., Wallace, K.A., McMillan, E.L., Zhang, S.C., and Gamm, D.M. (2009). Modeling early retinal development with human embryonic and induced pluripotent stem cells. Proc Natl Acad Sci U S A *106*, 16698-16703.

Najm, F.J., Chenoweth, J.G., Anderson, P.D., Nadeau, J.H., Redline, R.W., McKay, R.D., and Tesar, P.J. (2011). Isolation of epiblast stem cells from preimplantation mouse embryos. Cell stem cell *8*, 318-325.

Nichols, J., and Smith, A. (2009). Naive and primed pluripotent states. Cell stem cell *4*, 487-492.

Oliver, G., and Gruss, P. (1997). Current views on eye development. Trends in neurosciences *20*, 415-421.

Osakada, F., Ikeda, H., Mandai, M., Wataya, T., Watanabe, K., Yoshimura, N., Akaike, A., Sasai, Y., and Takahashi, M. (2008). Toward the generation of rod and cone photoreceptors from mouse, monkey and human embryonic stem cells. Nat Biotechnol *26*, 215-224.

Pankratz, M.T., Li, X.J., Lavaute, T.M., Lyons, E.A., Chen, X., and Zhang, S.C. (2007). Directed neural differentiation of human embryonic stem cells via an obligated primitive anterior stage. Stem Cells *25*, 1511-1520.

Pera, M.F., Andrade, J., Houssami, S., Reubinoff, B., Trounson, A., Stanley, E.G., Ward-van Oostwaard, D., and Mummery, C. (2004). Regulation of human embryonic stem cell differentiation by BMP-2 and its antagonist noggin. Journal of cell science *117*, 1269-1280.

Pollard, S.M., Benchoua, A., and Lowell, S. (2006). Neural stem cells, neurons, and glia. Methods Enzymol *418*, 151-169.

Reubinoff, B.E., Itsykson, P., Turetsky, T., Pera, M.F., Reinhartz, E., Itzik, A., and Ben-Hur, T. (2001). Neural progenitors from human embryonic stem cells. Nature biotechnology *19*, 1134-1140.

Schnapp, E., Kragl, M., Rubin, L., and Tanaka, E.M. (2005). Hedgehog signaling controls dorsoventral patterning, blastema cell proliferation and cartilage induction during axolotl tail regeneration. Development *132*, 3243-3253.

Strauss, O. (2005). The retinal pigment epithelium in visual function. Physiol Rev *85*, 845-881.

Takahashi, K., Tanabe, K., Ohnuki, M., Narita, M., Ichisaka, T., Tomoda, K., and Yamanaka, S. (2007). Induction of pluripotent stem cells from adult human fibroblasts by defined factors. Cell *131*, 861-872.

Takahashi, K., and Yamanaka, S. (2006). Induction of pluripotent stem cells from mouse embryonic and adult fibroblast cultures by defined factors. Cell *126*, 663-676.

Tesar, P.J., Chenoweth, J.G., Brook, F.A., Davies, T.J., Evans, E.P., Mack, D.L., Gardner, R.L., and McKay, R.D. (2007). New cell lines from mouse epiblast share defining features with human embryonic stem cells. Nature *448*, 196-199.

Thomson, J.A., Itskovitz-Eldor, J., Shapiro, S.S., Waknitz, M.A., Swiergiel, J.J., Marshall, V.S., and Jones, J.M. (1998). Embryonic stem cell lines derived from human blastocysts. Science *282*, 1145-1147.

Vugler, A., Carr, A.J., Lawrence, J., Chen, L.L., Burrell, K., Wright, A., Lundh, P., Semo, M., Ahmado, A., Gias, C*., et al.* (2008). Elucidating the phenomenon of HESC-derived RPE: anatomy of cell genesis, expansion and retinal transplantation. Exp Neurol *214*, 347-361.

Vukicevic, S., Kleinman, H.K., Luyten, F.P., Roberts, A.B., Roche, N.S., and Reddi, A.H. (1992). Identification of multiple active growth factors in basement membrane Matrigel suggests caution in interpretation of cellular activity related to extracellular matrix components. Experimental cell research *202*, 1-8.

Werb, Z., Tremble, P.M., Behrendtsen, O., Crowley, E., and Damsky, C.H. (1989). Signal transduction through the fibronectin receptor induces collagenase and stromelysin gene expression. The Journal of cell biology *109*, 877-889.

Yu, J., Vodyanik, M.A., Smuga-Otto, K., Antosiewicz-Bourget, J., Frane, J.L., Tian, S., Nie, J., Jonsdottir, G.A., Ruotti, V., Stewart, R*., et al.* (2007). Induced pluripotent stem cell lines derived from human somatic cells. Science *318*, 1917-1920.

Zegers, M.M., O'Brien, L.E., Yu, W., Datta, A., and Mostov, K.E. (2003). Epithelial polarity and tubulogenesis *in vitro*. Trends Cell Biol *13*, 169-176.

Zhang, S.C., Wernig, M., Duncan, I.D., Brustle, O., and Thomson, J.A. (2001). *In vitro* differentiation of transplantable neural precursors from human embryonic stem cells. Nature biotechnology *19*, 1129-1133.

Zhang, S.S., Fu, X.Y., and Barnstable, C.J. (2002). Molecular aspects of vertebrate retinal development. Molecular neurobiology *26*, 137-152.

Zuber, M.E., Gestri, G., Viczian, A.S., Barsacchi, G., and Harris, W.A. (2003). Specification of the vertebrate eye by a network of eye field transcription factors. Development *130*, 5155-5167.

Erklärung entsprechend 5.5 der Promotionsordnung/ Declaration according to 5.5 of the doctorate regulations

PhD Thesis Reconstitution of three-dimensional neuroepithelia from mouse and human pluripotent stem cells submitted by Yu Zhu

Hiermit versichere ich, dass ich die vorliegende Arbeit ohne unzulässige Hilfe Dritter und ohne Benutzung anderer als der angegebenen Hilfsmittel angefertigt habe; die aus fremden Quellen direkt oder indirekt übernommenen Gedanken sind als solche kenntlich gemacht. Die Arbeit wurde bisher weder im Inland noch im Ausland in gleicher oder ¨ahnlicher Form einer anderen Prüfungsbehörde vorgelegt.

Die Dissertation wurde von Prof. Dr. Elly M. Tanaka, Centre for Regenerative Therapies Dresden and Max-Planck-Institute for Molecular Cell Biology and Genetics, betreut und im Zeitraum vom 01/07/2008 bis 31/12/2011 verfasst.

Meine Person betreffend erkläre ich hiermit, dass keine früheren erfolglosen Promotionsverfahren stattgefunden haben.

Ich erkenne die Promotionsordnung der Fakultät für Mathematik und Naturwissenschaften, Technische Universität Dresden an.

I herewith declare that I have produced this paper without the prohibited assistance of third parties and without making use of aids other than those specified; notions taken over directly or indirectly from other sources have been identified as such. This paper has not previously been presented in identical or similar form to any other German or foreign examination board.

The thesis work was conducted from 01/07/2008 to 31/12/2011 under the supervision of Prof. Dr. Elly M. Tanaka at Centre for Regenerative Therapies Dresden and Max-Planck-Institute for Molecular Cell Biology and Genetics, in the laboratory of Prof. Dr. Elly M. Tanaka.

I declare that I have not undertaken any previous unsuccessful doctorate proceedings.

I declare that I recognize the doctorate regulations of the Fakultät für Mathematik und Naturwissenschaften of the Technische Universität Dresden.

Date Signature